

**AIRPLANE DYNAMIC MODELING
AND AUTOMATIC
FLIGHT CONTROL DESIGN**

by

Douglas E. Wolfe

Project submitted to the Faculty of the
Virginia Polytechnic Institute and State University
in partial fulfillment of the requirements for the degree of

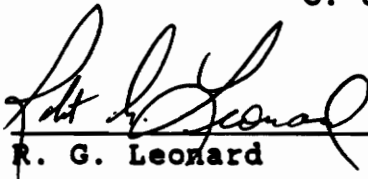
Master of Science

in

Systems Engineering

APPROVED:


C. J. Hurst, Chairman


R. G. Leonard


H. H. Robertshaw

February, 1990

Blacksburg, Virginia

C.2

LD
5655
VCS!
1990
10843
C.2

AIRPLANE DYNAMIC MODELING AND AUTOMATIC FLIGHT CONTROL DESIGN

by

Douglas E. Wolfe

Committee Chairman: Charles J. Hurst

Mechanical Engineering

(ABSTRACT)

This Systems Engineering project report discusses the design and implementation of automatic flight controls. The general airplane equations of motion are developed and used to calculate transfer functions for a Cessna 172 airplane. Automatic controllers were designed for four common autopilot modes (pitch control, altitude hold, roll control, and heading hold). Implementation of a flight control design was accomplished using single degree of freedom roll equations for a model airplane wing. The feedback compensation design was ground tested in a simulated wind tunnel and met performance requirements. All the elements of automatic flight control design are described in this report.

TABLE OF CONTENTS

<u>Section</u>	<u>Page</u>
Chapter 1: Introduction	1
Chapter 2: Transfer Functions and Compensator Design	
2.1 Airplane Model	4
2.2 Airplane Transfer Functions	11
2.3 Stability Analysis and Compensator Design . . .	17
Chapter 3: Implementation of Control System Design	38
3.1 Simplified Motion Equations for Single DOF Wing	39
3.2 Test hardware Description	40
3.3 Experimental Parameter Determination	44
3.4 Project Performance Specifications	48
3.5 Compensator Design	49
3.6 System Test Results	56
Chapter 4: Summary and Conclusions	
4.1 Project Conclusions	57
4.2 Suggestions for Further Study	58
References	59
Appendix 1: Example Airplane Flight Conditions . . .	60
Appendix 2: Longitudinal Transfer Functions	61
Appendix 3: Lateral Transfer Functions	67

Chapter 1: INTRODUCTION

Airplanes and spacecraft are excellent examples of systems requiring feedback control for operation. In airplanes the feedback and compensation functions are often provided by the pilot; however, an autopilot control system is created when the plane's position or rate is sensed and control surfaces actuated to meet given performance specifications. A prerequisite for autopilot design is that the airplane as a plant must be inherently stable, or have a feedback mechanism that provides stability, in order for its response to disturbances and changes in control surfaces to result in stable steady-state flight conditions. Autopilot systems sometimes replace humans for safety purposes as in reduced visibility landings. Also as sensing elements, (gyroscopes, altimeters, etc.) became more sophisticated and military needs such as stealth and advanced fighters emerged, the requirement for faster response times increased and automatic control systems became necessary. [1, pg. 453]*

The subject of aerodynamic stability and control deals with the reaction of the airplane to internally or externally generated disturbances.

* Numbers in square brackets, [], refer to references

Examples of internal disturbances are changes in rudder, aileron, or elevator control surfaces; changes in center of gravity location; and changes in airplane configuration (i.e., flaps extension, landing gear up or down, etc.). External disturbances are atmospheric turbulence, upset gusts, and changes in altitude and temperature. The response of the airplane to the disturbances is the change with time of motion variables relative to some steady-state flight condition. Stability criteria are selected to describe the required airplane response to the perturbed motion. As a result, a transfer function is required which describes the relationship of airplane motion to a control surface deflection. [2, pg. 1]

This project was undertaken to develop an understanding of airplane dynamic models and transfer functions, to design autopilots, and to build hardware to implement a control system design. To meet these objectives, the project was divided into two parts. Part one consisted of developing theoretical airplane models and using these models to design feedback control systems. An example airplane was selected with a specific set of geometries and flight conditions and the transfer functions developed for this system. Feedback control systems were designed for several autopilot control modes. The second part of the project used the theory derived in part one and applied it to the design of a single degree-

of-freedom roll problem. The wing section from a radio control airplane was attached to a platform providing the roll axis motion. A feedback control system was designed to maintain the wing at a desired bank angle. The control system implemented a simple compensation circuit.

This project report format follows the approach described in the above paragraph. In summary there are two primary objectives for this project. These are:

1. Develop generalized formulas for determining airplane transfer functions, and to use these transfer functions to design automatic control systems for a specific airplane to meet a given set of performance specifications.
2. Using a radio control model airplane, design, build, and test a compensation system to automatically control the airplane's roll mode.

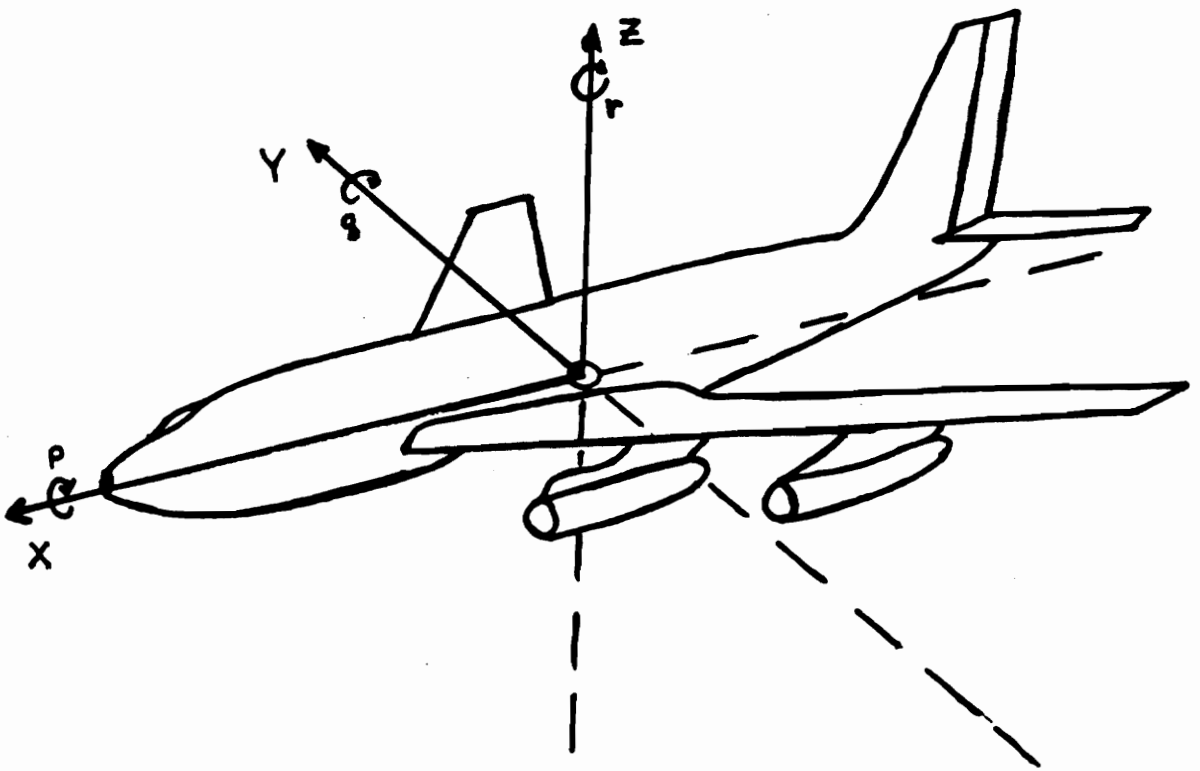
Chapter 2: TRANSFER FUNCTIONS AND COMPENSATOR DESIGN

2.1 Airplane Model

The initial step in designing a control system is to develop an accurate mathematical model of the system. This section will develop the equations of motion and describe the variables and constants used in this equation. It will also specify a coordinate system most useful for analysis and will evaluate the aerodynamic derivatives used in the equations.

In developing equations of motion, the most convenient coordinate system to use is the stability axis system. Figure 1 defines the airplane axis system and motion variables. [3, pg. 4] Consider an airplane flying a symmetrical steady state straight line flight path. [2, pg. 113] That means $p=q=r=v=0$ but u and w are not zero. The angle between the free stream velocity vector V_{∞} and U_1 is called α , the steady state angle of attack. The stability axes are obtained from the body axes by rotating about the Y axis over an angle α until X coincides with V_{∞} . Figure 2 illustrates this procedure. The new axis system is considered to be rigidly attached to the airplane and moves with the airplane. The stability axis system has been chosen with respect to a particular steady state flight condition. In the case of an airplane where V is not equal zero, the airplane is said to be sideslipping. The sideslip angle is defined as β . The X axis of the stability system lies along the projection of

Axis	Force Along	Moment About	Linear Velocity
X	F_x	L	u
Y	F_y	M	v
Z	F_z	N	w



Axis	Angular Displacement	Angular Velocity	Inertia
X	ϕ	p	I_x
Y	θ	q	I_y
Z	psi	r	I_z

Figure 1: Airplane Axis System

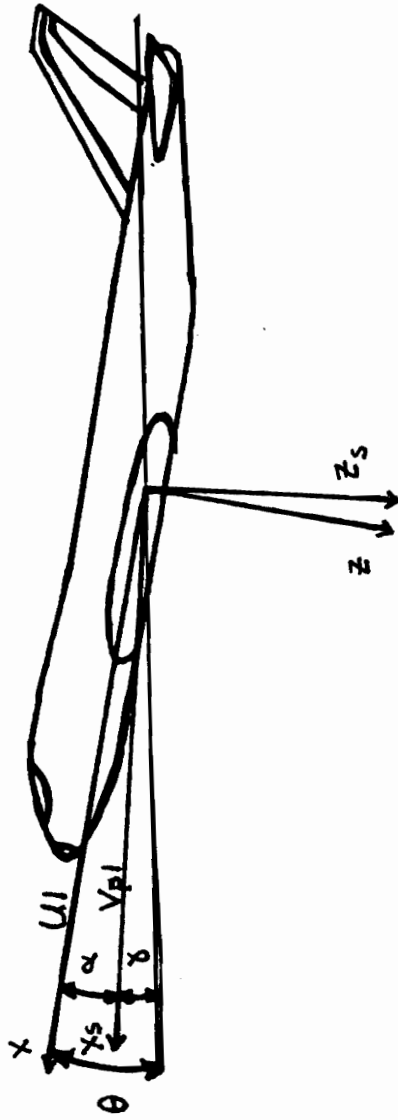


Figure 2: Stability Axis System

the steady state velocity vector in the XZ plane. All equations of motion used in this project are determined in stability axis coordinates. The equations of motion make use of dimensional and nondimensional aerodynamic derivatives. The nondimensional derivatives describe thrust, drag, and lift forces as a function of the airplane geometry and the effects of control surface deflection. References 1 through 4 all discuss the determination of these derivatives. The definitions of the dimensional derivatives are given in Appendices 2 and 3. These derivatives are acceleration quantities per unit of the associated motion variable. For example, X_u is the forward acceleration in ft./sec.² per unit change in forward speed u (ft/sec.).

Using the above developed derivatives, the airplane equations of motion can be written as shown in Tables 1 and 2. There are six equations that describe the forces and moments about the X, Y, and Z axes respectively. [2, pgs. 414 & 446] The equations are linearized by assuming that all perturbation quantities such as δv , $\delta \alpha$, etc. are small and that the squares and products of these quantities can be neglected. Also, the equations are divided into longitudinal and lateral equations. The longitudinal equations describe forces along the X and Z axes and moments about the Y axis. The lateral equations describe force along the Y axis and moments about the X and Z axes. Using

Table 1: Longitudinal Small Perturbation Equations

$$\dot{u} := -g \cdot \theta \cdot \cos(\theta) + X_u \cdot u + X_{tu} \cdot \dot{u} + X_\alpha \cdot \alpha + X_{\delta E} \cdot \delta E$$

$$\dot{w}_1 := U \cdot q + -g \cdot \theta \cdot \sin(\theta) + Z_u \cdot u + Z_\alpha \cdot \alpha + Z_{\dot{\alpha}} \cdot \dot{\alpha}$$

$$\dot{w} := \dot{w}_1 + Z_q \cdot q + Z_{\delta E} \cdot \delta E$$

$$\dot{q} := M_u \cdot u + M_{tu} \cdot \dot{u} + M_\alpha \cdot \alpha + M_{t\alpha} \cdot \dot{\alpha} + M_{\dot{\alpha}} \cdot \dot{\alpha} + M_q \cdot q + M_{\delta E} \cdot \delta E$$

Aerodynamic Derivatives:	X_u	X_{tu}	X_α	$X_{\delta E}$
	Z_u	Z_α	Z_q	$Z_{\delta E}$
	$M_{\delta E}$	M_u	M_{tu}	M_α
			$M_{\dot{\alpha}}$	M_q

δE = Elevator deflection

θ = Pitch rotation angle

α = attitude angle

u = forward velocity

w = vertical velocity

\dot{q} = pitch rotation velocity

Table 2: Lateral Small Perturbation Equations

$$\dot{v} := -U \cdot \dot{r} + g \cdot \phi \cdot \cos(\theta) + Y_{\beta} \cdot \beta + Y_p \cdot p + Y_r \cdot r + Y_{\delta A} \cdot \delta A$$

$$\dot{p} := A1 \cdot \dot{r} + L_{\beta} \cdot \beta + L_p \cdot p + L_r \cdot r + L_{\delta A} \cdot \delta A + L_{\delta R} \cdot \delta R$$

$$\dot{r} := B1 \cdot \dot{p} + N_{\beta} \cdot \beta + N_{T\beta} \cdot \beta + N_p \cdot p + N_r \cdot r + N_{\delta A} \cdot \delta A$$

$$A1 := \frac{I_{xz}}{I_{xx}}$$

$$B1 := \frac{I_{xz}}{I_{zz}}$$

Aerodynamic Derivatives:

	Y_{β}	Y_p	Y_r	$Y_{\delta A}$	$Y_{\delta R}$	
	L_{β}	L_p	L_r	$L_{\delta A}$	$L_{\delta R}$	
	N_{β}	$N_{T\beta}$	N_p	N_r	$N_{\delta A}$	$N_{\delta R}$

 ϕ = Roll angle δA = aileron deflection β = sideslip angle δR = rudder deflection ψ = heading angle \dot{p} = roll rate \dot{r} = rotation about vertical axis \dot{v} = lateral velocity

conventional aerodynamic assumptions concerning the force and moment terms, the equations completely decouple into two independent sets. These assumptions are in [4, pg. 160]:

1. The derivatives of the asymmetric or lateral forces and moments with respect to the symmetric or longitudinal variables are zero.

2. All derivatives of the symmetric forces and moments with respect to the asymmetric motion variables may be neglected.

3. All derivatives with respect to rates of change of motion variables except for $L_{\dot{\alpha}}$ and $M_{\dot{\alpha}}$ may be neglected.

These equations are in a suitable form for transfer function determination and subsequent control system analysis.

2.2 Airplane Transfer Functions

As developed in section 2.1, the airplane equations of motion can be written in the form of transfer functions which will describe airplane response due to control surface deflections. In this section, these equations will be used to determine a set of transfer functions for a specific airplane, and the control system design discussed in section 2.3 will be performed for this airplane.

After taking the Laplace transform of the equations in Tables 1 and 2, the equations were arranged in matrix form as a function of motion variable versus control surface deflection. Tables 3 and 4 show these equations. [2, pgs. 414 & 446] Longitudinal modes can be described by the airplane response to elevator deflections while lateral modes are a function of aileron and rudder deflections. Solutions for the transfer functions are obtained using Cramer's rule. These transfer functions are written using dimensional derivatives. The dimensional derivatives can be evaluated by using the characteristics of a particular airplane and flight condition.

The airplane selected is representative of a small four-place personal transportation airplane (i.e., Cessna 172). Stability and control derivatives, flight conditions, geometries and inertias, and steady state coefficients are given for this airplane in [2, pg. 591] Appendix 1 contains these values.

Table 3: Longitudinal Transfer Function Determination

$$A := \begin{bmatrix} s - X & -X \\ u & tu \\ -Z & \alpha \\ M + M & -[M \cdot s + M + M] \\ tu & \alpha \dot{\alpha} \end{bmatrix} \begin{bmatrix} -X \\ \alpha \\ -Z \\ \alpha \dot{\alpha} \end{bmatrix} - \begin{bmatrix} -Z \\ \alpha \\ \alpha \dot{\alpha} \end{bmatrix} \begin{bmatrix} g \cdot \cos(\theta) \\ s + U \\ q \end{bmatrix} \begin{bmatrix} s - M \cdot s \\ q \end{bmatrix}$$

$$\begin{bmatrix} X \\ \delta E \\ Z \\ \delta E \\ M \\ \delta E \end{bmatrix} := A \cdot \begin{bmatrix} U \\ \alpha \\ \theta \end{bmatrix} \cdot \frac{1}{\delta} E$$

Using Cramer's rule, the transfer functions for U, α , and θ as a function of elevator deflection can be determined.

Table 4: Lateral Transfer Function Determination

$$C := \begin{bmatrix} \begin{bmatrix} s \cdot U - Y \\ \beta \end{bmatrix} & - \begin{bmatrix} s \cdot Y + g \cdot \cos(\theta) \\ P \end{bmatrix} & s \cdot \begin{bmatrix} U - Y \\ r \end{bmatrix} \\ -L & \begin{bmatrix} s - L \cdot s \\ P \end{bmatrix} & - \begin{bmatrix} s \cdot A1 + s \cdot L \\ r \end{bmatrix} \\ -N - N_{T\beta} & - \begin{bmatrix} s \cdot B1 + N \cdot s \\ P \end{bmatrix} & \begin{bmatrix} s - s \cdot N \\ r \end{bmatrix} \end{bmatrix}$$

Note: Substitute δR for rudder deflection

$$\begin{bmatrix} Y \\ \delta A \\ L \\ \delta A \\ N \\ \delta A \end{bmatrix} := C \cdot \begin{bmatrix} \beta \\ \psi \end{bmatrix} \cdot \frac{1}{\delta A}$$

As in longitudinal case, use of Cramer's rule will determine lateral transfer functions

Appendices 2 and 3 contain the equations for determining the transfer function for the lateral and longitudinal modes. [2, ch. 6] Flight conditions for both modes were the same. A Mathcad program was used to implement the example airplane data into the equations of motion and develop the transfer functions. An equation-solving feature of Mathcad was used to find the pole and zero values for each equation. Tables 5 and 6 contain the resulting longitudinal and lateral transfer functions in polynomial form.

This developed model is applied to a specific airplane; however, by using different flight conditions, geometries, and/or nondimensional derivatives a new set of transfer functions can be determined. For a complete control system design, a sensitivity analysis would be required to insure that performance was satisfactory over the desired range of flight conditions for the respective airplane. The program developed would be capable of handling this type of analysis.

Table 5: Example Airplane Longitudinal Transfer Functions

$$u := -6.25 \cdot \frac{s^3 + 8.87s^2 - 48.4s - 418.9}{s^4 + 8.31s^3 + 36.7s^2 + 1.8s + 1.2} \cdot \delta E$$

$$\alpha := -.202 \cdot \frac{s^3 + 195.2s^2 + 8.46s + 8.43}{s^4 + 8.31s^3 + 36.7s^2 + 1.8s + 1.2} \cdot \delta E$$

$$\theta := -39.5 \cdot \frac{s^2 + 2.11s + .12}{s^4 + 8.31s^3 + 36.7s^2 + 1.8s + 1.2} \cdot \delta E$$

$$h := .202 \cdot \frac{s^3 - .35s^2 - 403s - 15.1}{s^4 + 8.31s^3 + 36.7s^2 + 1.8s + 1.2} \cdot \delta E$$

Table 6: Example Airplane Lateral Transfer Functions

$$\beta := 30.9 \cdot \frac{s^2 + 16.3s + .94}{s^4 + 13.8s^3 + 28.6s^2 + 142.3s + 1.6} \cdot \delta A$$

$$\phi := 57.5 \cdot \frac{s^2 + 1.04s + 6}{s^4 + 13.8s^3 + 28.6s^2 + 142.3s + 1.6} \cdot \delta A$$

$$\psi := 31.4 \cdot \frac{-s^3 - 15.2s^2 - 2.3s + .0006}{s^4 + 13.8s^3 + 28.6s^2 + 142.3s + 1.6} \cdot \delta A$$

$$\beta := .089 \cdot \frac{s^3 + 127s^2 + 146s - 32.9}{s^4 + 13.8s^3 + 28.6s^2 + 142.3s + 1.6} \cdot \delta R$$

$$\phi := 4.75 \cdot \frac{s^2 - 5.6s - 52.2}{s^4 + 13.8s^3 + 28.6s^2 + 142.3s + 1.6} \cdot \delta R$$

$$\psi := -10.2 \cdot \frac{s^3 + 12.6s^2 + .6s + .004}{s^4 + 13.8s^3 + 28.6s^2 + 142.3s + 1.6} \cdot \delta R$$

2.3 Stability Analysis and Compensator Design

The previous airplane model development and transfer functions determination make possible the design of automatic (autopilot) control systems. In this section, four common autopilot modes are designed for the example airplane described in section 2.2. For the longitudinal case, a pitch attitude hold and an altitude hold mode were designed. In the lateral case, a bank angle hold/wing leveler and heading hold mode autopilot were designed. The wing leveler autopilot is the design implemented in part two of the project. The goal was to find autopilot designs that would meet or best approximate a set of design specifications. The computer program "CC" was an important tool used in the analysis. This program plots root locus diagrams, frequency response curves, and time response performance among other things.

The following design specifications are requirements for the autopilot systems. [2, ch. 11] The specifications are divided into three parts: frequency response, time response, and error specifications.

Frequency Response;

- $M_p < 1.7$ db. closed loop
- Phase Margin > 35 degrees
- Gain Margin > 9.5 db
- Damping (phugoid) $> .04$
- Damping (short period) $.30 < D_{sp} < 2.0$

- Time Domain; - Overshoot < 10%
- Rise Time (10% to 90%) < 3 sec.
- Steady State Error < 10%
- Error Specifications; - $K_p > 9$, $E_p < .1$
- $K_v > .1$, $E_v < 10$

These specifications were determined from requirements stated in reference 2.

The same design approach was used for all autopilot modes. System performance can be described by the following equation:

$$y(s) = G/(1+G)*r(s) + 1/(1+G)*d(s) - G/(1+G)*n(s) \quad 2.1$$

where G describes the plant, $r(s)$ is the reference input, $d(s)$ is a disturbance applied to the output $y(s)$, and $n(s)$ is sensor noise resident in the system feedback loop. [5, pg. 46] Performance is good if the output $y(s)$ approximates a command input $r(s)$, rejects a disturbance in the output and rejects sensor noise. By considering the magnitude of $G(j\omega)/(1+G(j\omega))$, $1/(1+G(j\omega))$, and $-G(j\omega)/(1+G(j\omega))$, high gain provides good output command following and disturbance rejection but does not reject sensor noise. All of these objectives can be achieved by providing high gain at low frequencies and low gain at high frequencies. This assumes high frequency sensor noise. By including an integrator in $G(s)$, there will be zero steady state error to a step input and also high gain at low frequencies. This approach was used

for all autopilot designs.

The characteristic equation in the denominator of the longitudinal transfer functions is fourth order and consists of two oscillatory modes. These modes are referred to as the phugoid and short period modes. The phugoid mode takes place at constant angle of attack, and the short period modes takes place at constant speed. To simplify control system design, it is customary to consider these two modes leaving out the alpha and u equations respectively. [4, pg. 456] This is done to simplify the analysis, but will not be necessary here given the availability of the "CC" program.

For the example airplane, the short period and phugoid modes are characterized as follows:

<u>Mode</u>	<u>Polynomial</u>	<u>Natural Frequency</u>	<u>Damping</u>
Phugoid	$s^2 + .042s + .032$	$w = .179 \text{ rad/sec.}$.117
short period	$s^2 + 8.26s + 36.7$	$w = 6.03 \text{ rad/sec.}$.684

Pitch Attitude Hold: The transfer function defining the change in theta as a function of elevator deflection applies to this mode. As noted above, the short period damping of the example airplane meets the requirement; however, pitch attitude hold modes frequently require an inner loop rate feedback. This has the effect of artificially increasing the system stiffness. The pitch damper moves the closed loop

poles into a region where the damping is improved and gives the advantage of greater gain in the outer loop. A pitch damper, or stability augmentation system, was added here to illustrate this procedure. Rate was determined by differentiating position. Using this transfer function and a servo transfer function given in [2, pg. 1089] of $10/(s+10)$, an inner loop system was designed that reduced the closed loop peak magnitude response by a factor of 2. [2, pg. 1102]

The stability augmentation system was included in the design of the pitch position autopilot. Pitch rate was integrated to give pitch position as the output. A vertical gyro was included in the feedback loop with a gain of 1. To be consistent with the design approach, the compensator selected required an integrator for frequency loop shaping. Consequently, a proportional, integral, differential (PID) compensator was used. The effect of the PID compensator was to provide two arbitrarily placed open and closed loop zeros while introducing an integrator in the denominator to create a type 1 system. The initial PID settings were found using Ziegler-Nichols methods. [6, pg. 343] The integrator causes an increase in system oscillation and peak overshoot, but by adding differential control and sensing the rate of change of the actuating signal, the oscillatory behavior can be reduced. Also, the PID controller maintains the phase at less than 180 degrees throughout the system bandwidth. This

increased bandwidth allows a wider range of controller gain settings to meet desired performance requirements.

Figures 3 through 6 contain the open and closed loop Bode plots, the root locus, and time response diagrams. Figure 7 shows the entire pitch control system. The PID controller gain is negative due to the negative gain in the transfer function. The performance parameters for all autopilot designs are included in Table 7 at the end of Section 2.3, pg. 37. As shown by the open loop Bode plot, the gain at low frequency is high and there is zero error in the steady state time response. The phugoid and short period modes can be seen in the magnitude curve on the open loop Bode plot. The controller design meets all requirements for the given flight conditions. In actual practice, the performance would have to be considered over a full range of altitudes, attitudes, and disturbances.

Altitude Hold: The altitude hold is frequently found in many autopilots. Altitude is given by h and the rate of climb is:

$$\dot{h} = U * \sin(\gamma) \cong U * \gamma \quad 2.2$$

γ is the angle from the horizon to the forward velocity vector of the airplane. α is the angle from the velocity vector to the airplane attitude. θ is the sum of these two angles. Using this relationship, taking the Laplace transform of equation 2.2 and using elevator control, the

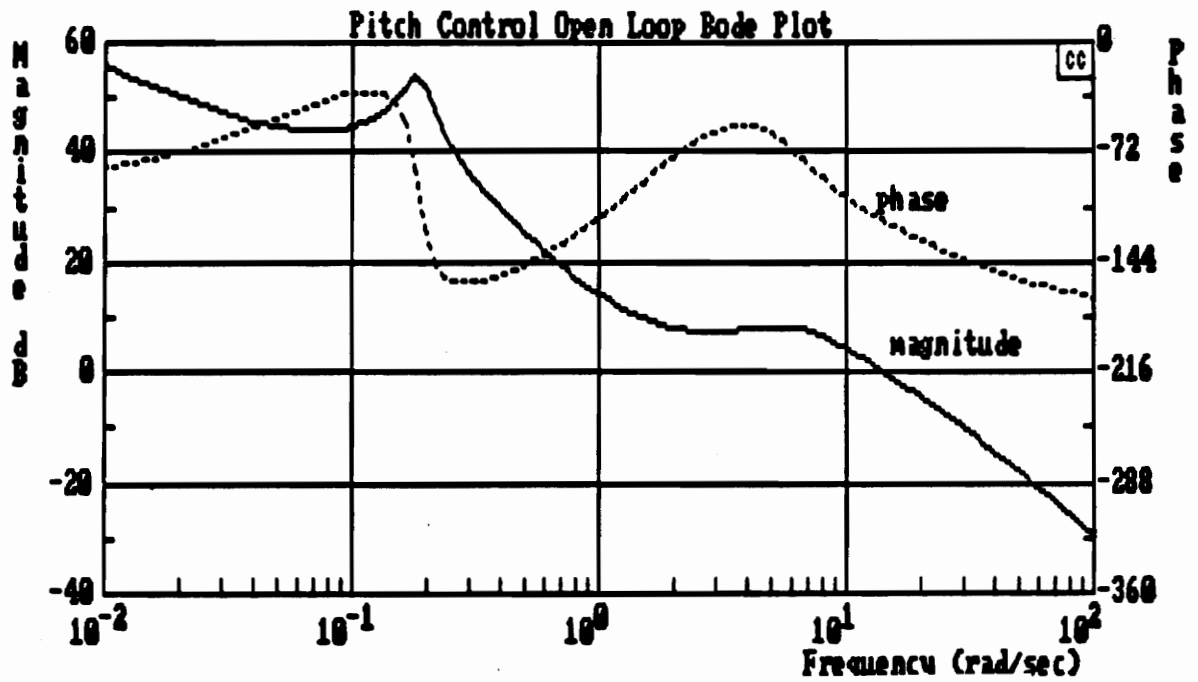


Figure 3: Pitch Control Open Loop Bode Plot

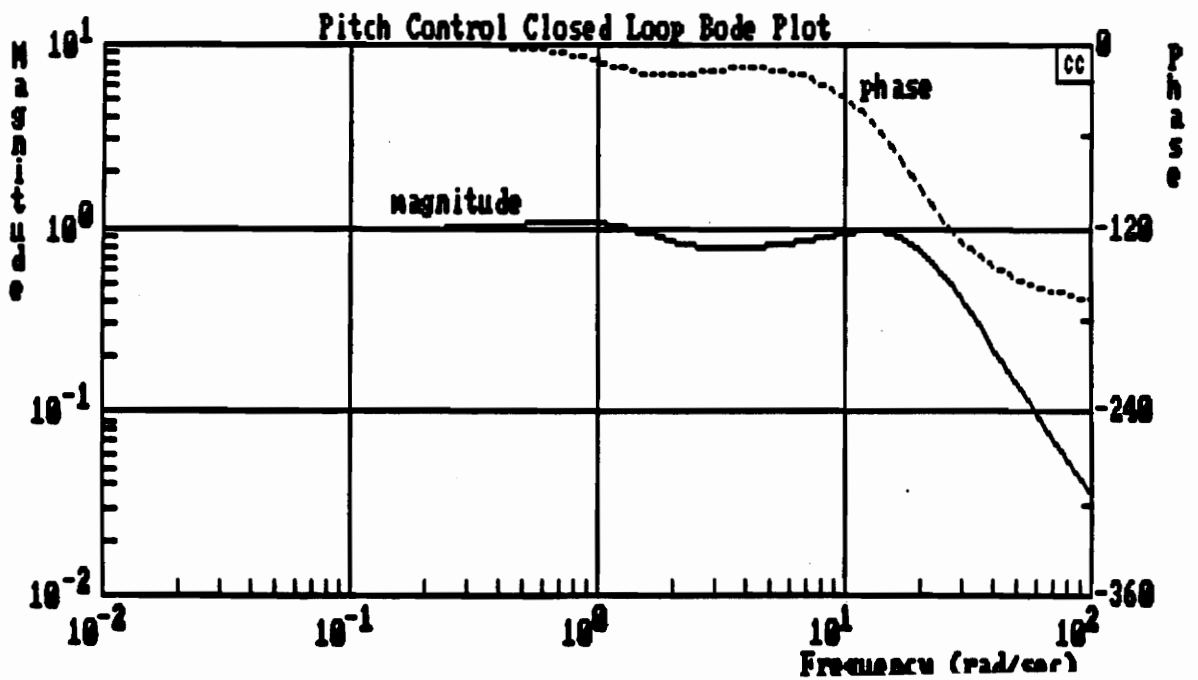


Figure 4: Pitch Control Closed Loop Bode Plot

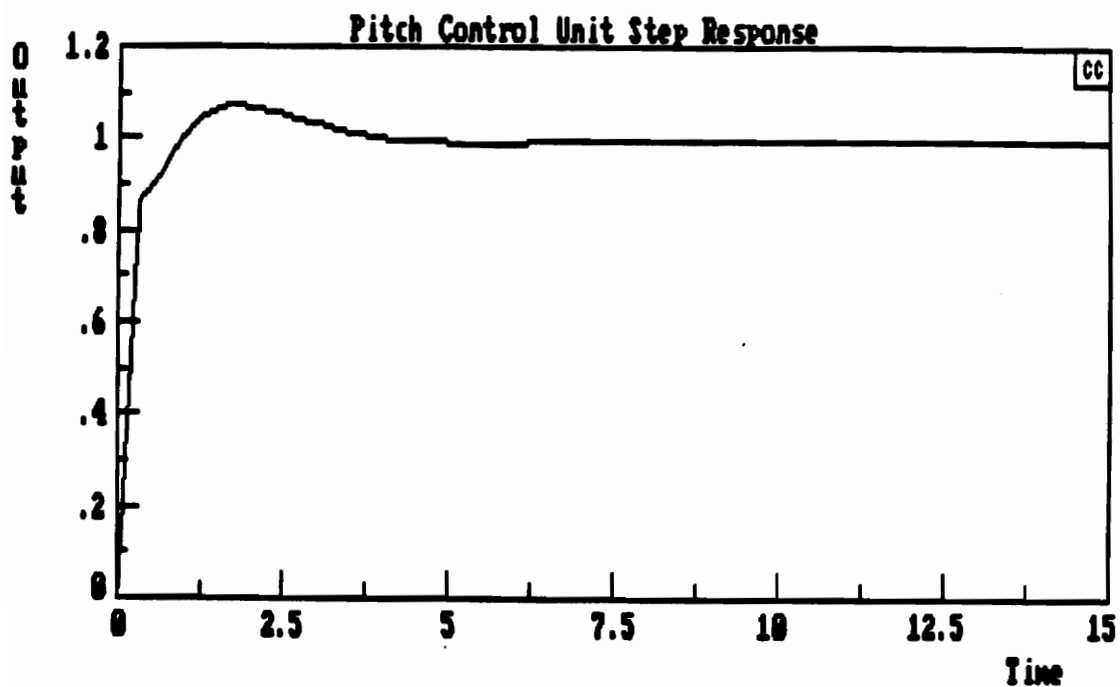


Figure 5: Pitch Control Unit Step Response

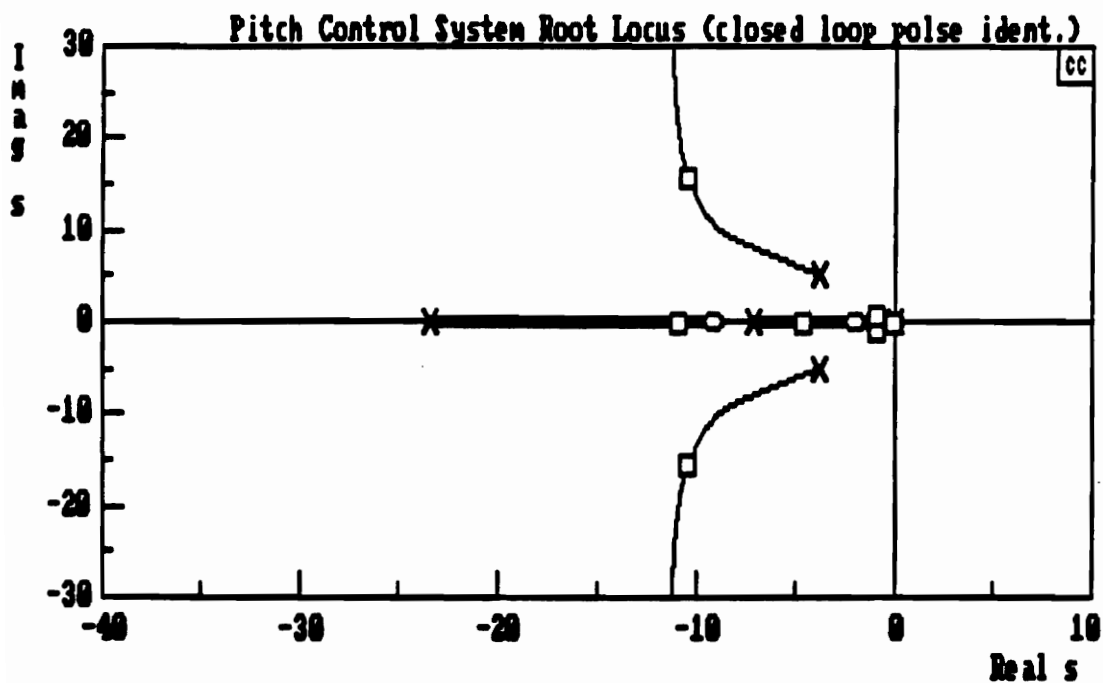


Figure 6: Pitch Control System Root Locus

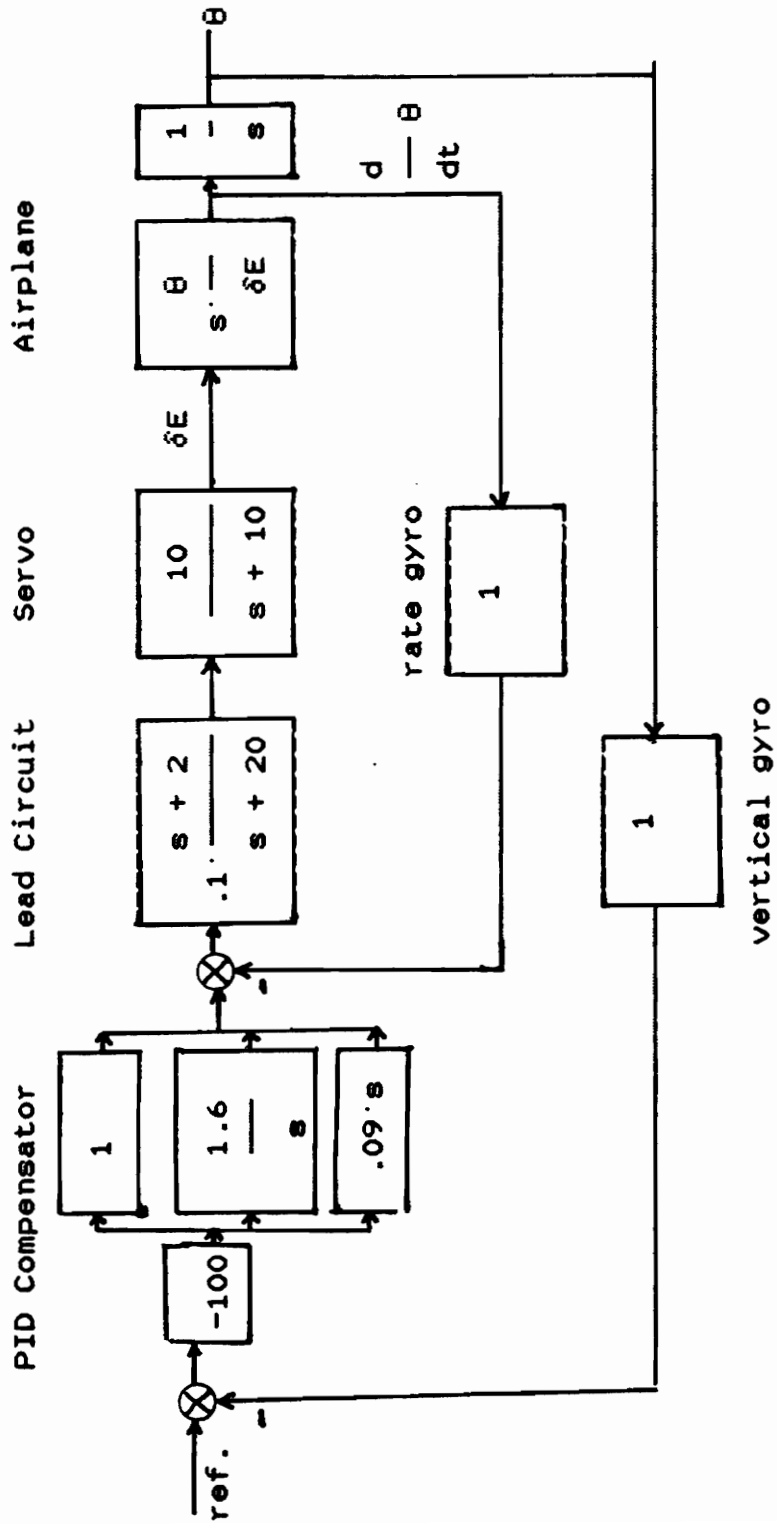


Figure 7: Pitch Control Mode

altitude to elevator deflection transfer function can be determined:

$$h(s)/\text{elev.}(s) = U/s *(\theta(s) - \alpha(s))/\Delta e(s) \quad 2.3$$

Altitude is a long term navigational requirement and requires that the phugoid mode be considered. Using equation 2.3, the transfer function for altitude versus elevator deflection was found and included in Table 5, pg. 15. [2, pg. 1141]

Given the transfer function from equation 2.3, the altitude hold autopilot was designed. The servo equation used was again $10/(s+10)$, and an altimeter with unity gain was the feedback mechanism. Figures 8 through 11 contain the response curves and Figure 12 shows the altitude hold autopilot design. An integrator was introduced in the compensator to create a type 1 system. The root locus diagram shows that the system is close to going unstable. To obtain the root locus shown, one arbitrary zero was selected and the gain set to place the closed loop poles. This design caused a peak overshoot of 20% in the time response but the rise time requirement was satisfied. The closed loop magnitude peak was .5 db. greater than specified. A design tradeoff can be made by reducing the gain to improve the overshoot and peak magnitude and accepting a slower rise time. Again the phase is less than 180 degrees for the entire system bandwidth and will allow variations in gain settings. As shown in Table 7, pg. 37, all other parameters were achieved with this design.

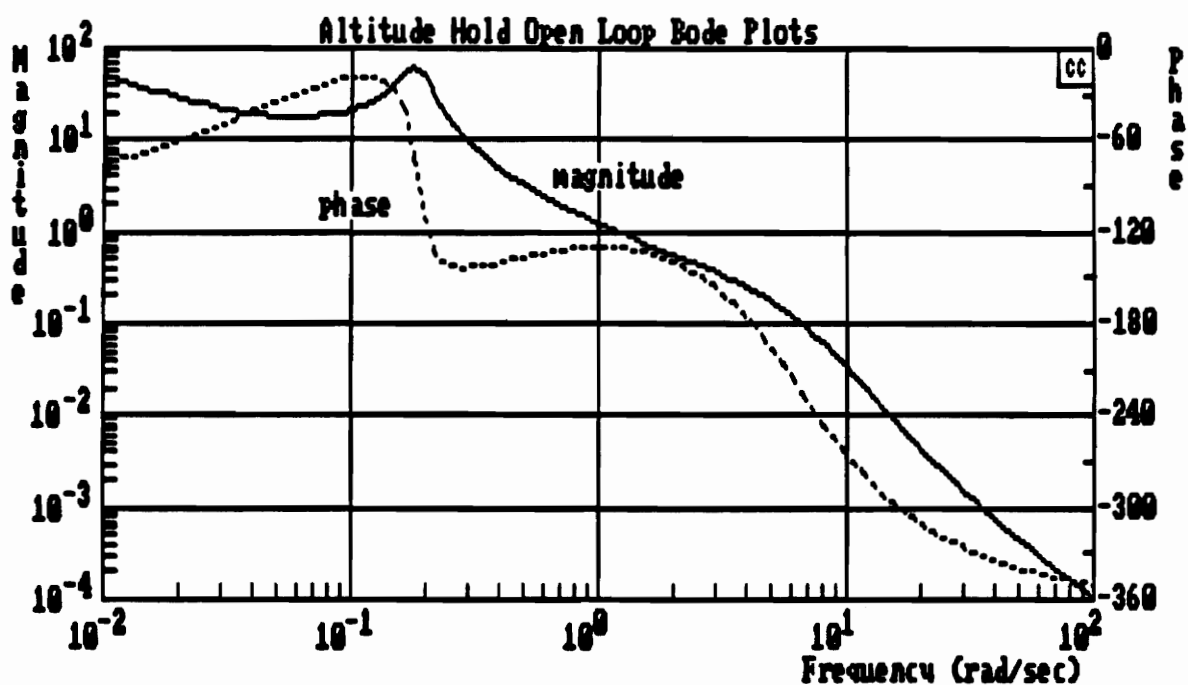


Figure 8: Altitude Hold Open Loop Bode Plot

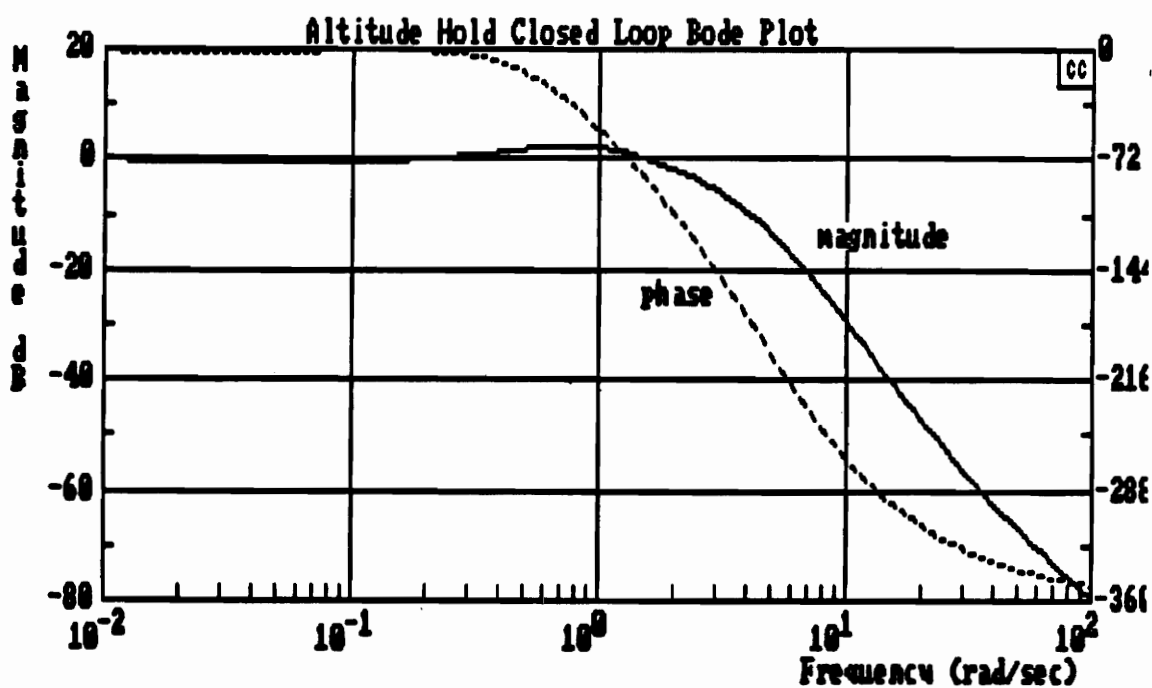


Figure 9: Altitude Hold Closed Loop Bode Plot

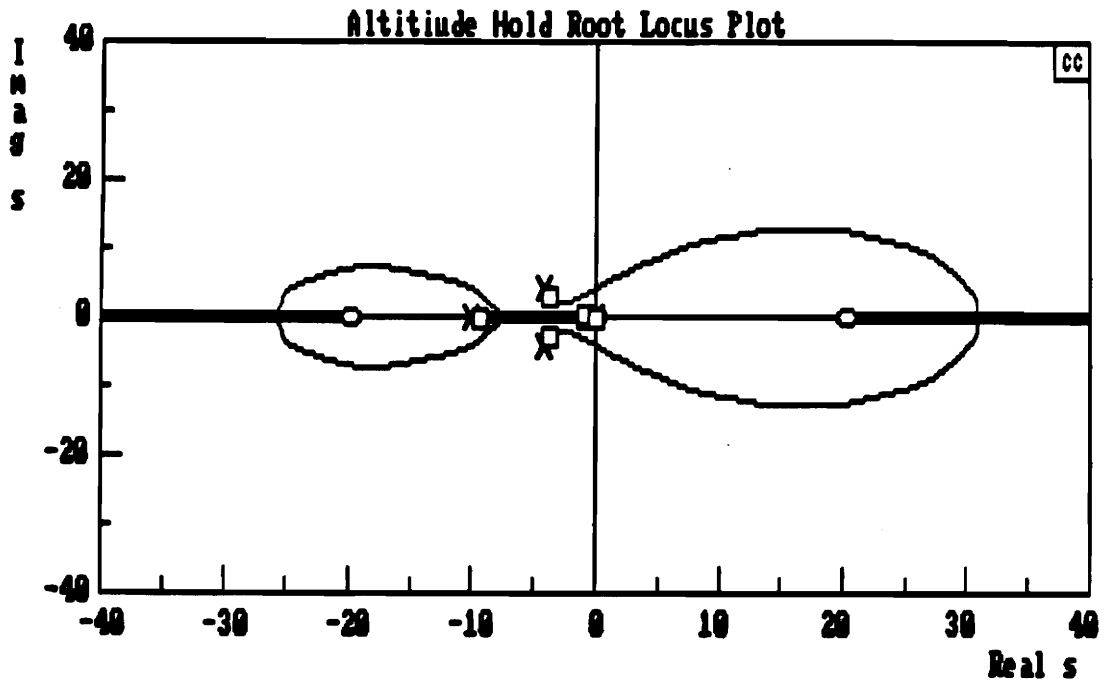


Figure 10: Altitude Hold Root Locus

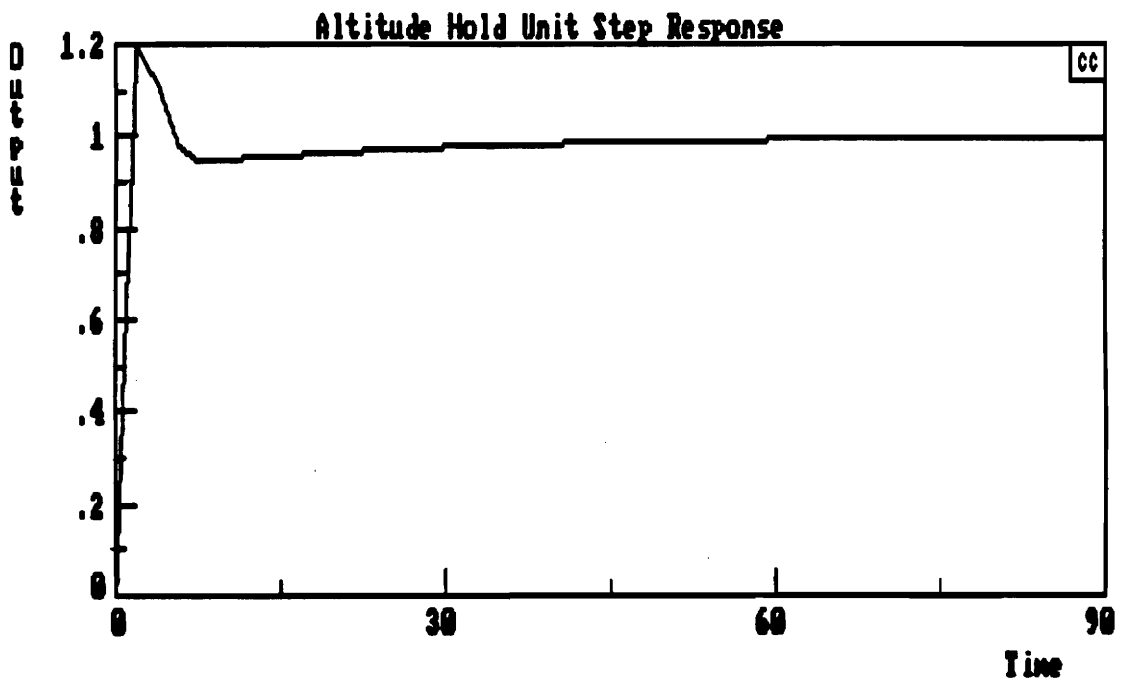


Figure 11: Altitude Hold Unit Step Response

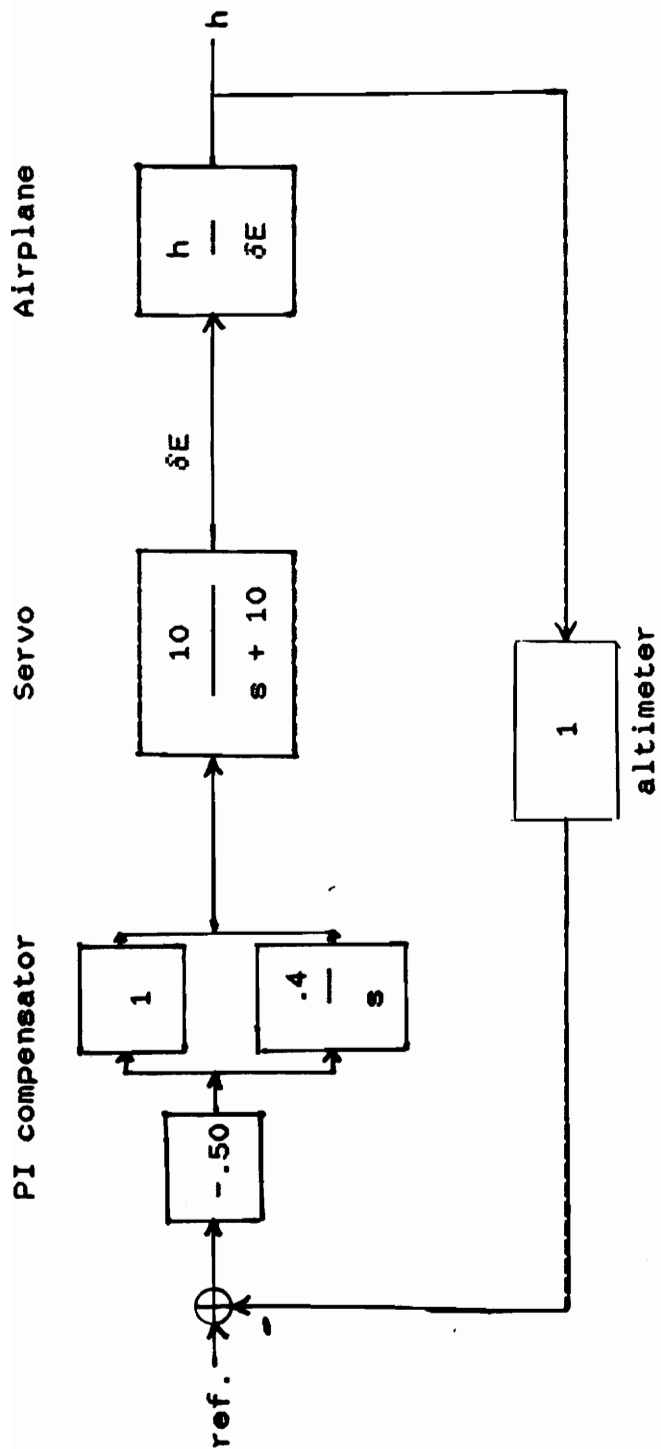


Figure 12: Altitude Hold Mode

As in the longitudinal case, the lateral characteristic equation in the transfer function denominator is fourth order. This equation is made up of one oscillatory pair of roots and two real roots. The two real roots describe the spiral mode and the rolling mode of motion. The slowly damped low frequency oscillation is called the dutch roll mode. The spiral mode is dominated by the bank angle and heading angle. The roll mode can be approximated by a single degree of freedom roll equation. The dutch roll consists primarily of sideslipping and yawing and the roll term can be eliminated. The analysis done here used the full characteristic equation. [4, ch. 7]

For the example airplane, the lateral modes are described as follows:

<u>Mode</u>	<u>Polynomial</u>	<u>Natural Frequency</u>	<u>Damping</u>
Dutch roll	$s^2 + 1.4s + 11.4$	3.37 rad/sec.	.203
Spiral	$s + .011$	$T_s = 90.9$ sec.	NA
Roll	$s + 12.5$	$T_r = .08$ sec.	NA

Bank Angle hold/wing leveler: This autopilot mode is used to control the airplane roll angle, ϕ . The calculations included all modes of the transfer function, not just the first order approximation. As in the longitudinal cases, the $10/(s+10)$ servo was used. For some airplanes and

flight conditions, it may be necessary to include an inner loop stability augmentation system; however, this was not required for the example airplane.

The design chosen here used a proportional-differential (PD) controller. This controller places an open and closed loop zero in the system and has the effect of reducing the peak overshoot and settling time. The zero also provides a phase lead. The zero chosen for this system was at $s=9$. Figures 13 through 16 show the system response curves, and Figure 17 shows the autopilot design. As shown in the open loop Bode plot, an integrator was not required for frequency loop shaping. An integrator is added for the heading hold mode in the next section. Table 7 shows that all response requirements were achieved by the closed loop PD design.

Heading hold: Using the bank angle hold design found above, a heading hold autopilot was designed. The relationship between bank angle and heading is given by:

$$\dot{\psi} = g * \tan(\phi) / (U) \approx g*\phi/(U) \quad 2.4$$

Taking the Laplace transform gives:

$$\psi(s) = g * \phi(s) / (U * s) \quad 2.5$$

Using equation 2.5, a heading hold autopilot was designed. As seen earlier in Figure 17, the heading hold design used a heading gyro for feedback and a proportional control compensator. Figures 18 through 21 show the system response curves. The proportional design was selected from the time

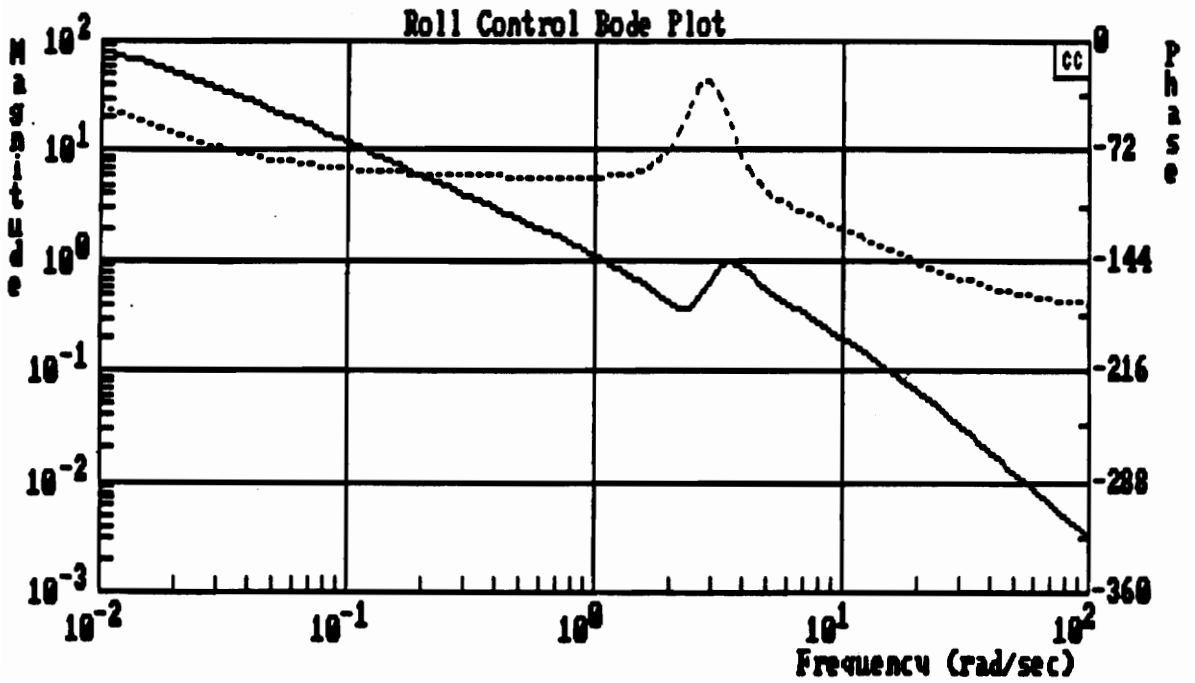


Figure 13: Roll Control Bode Plot

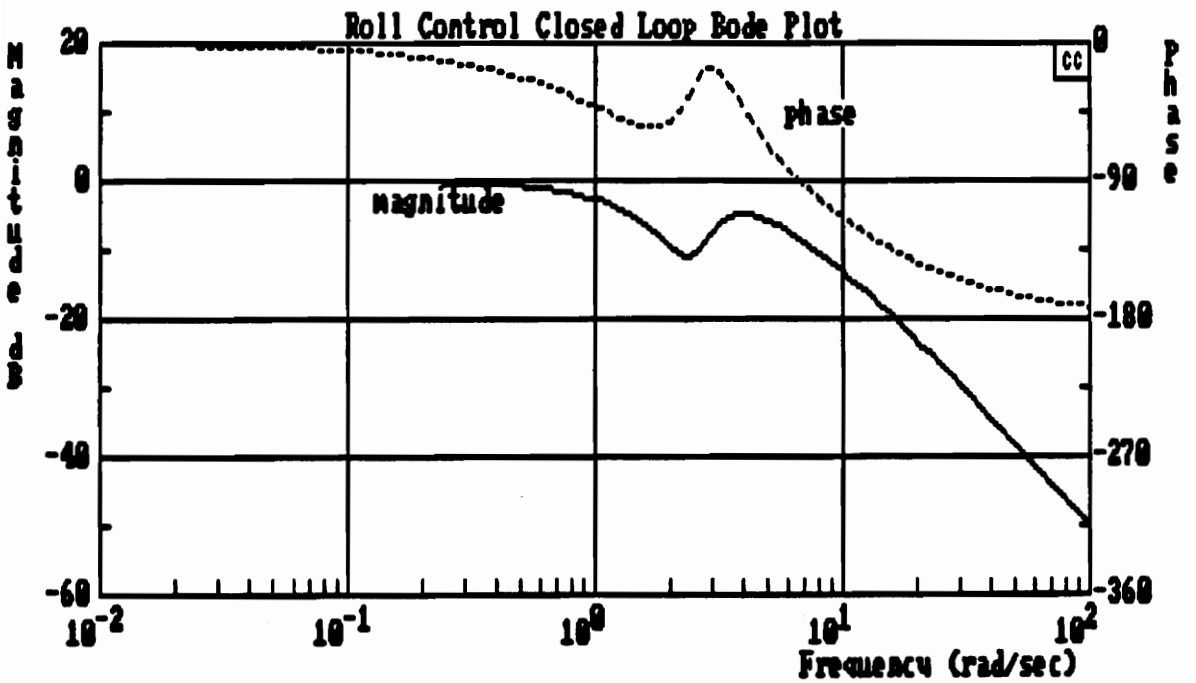


Figure 14: Roll Control Closed Loop Bode Plot

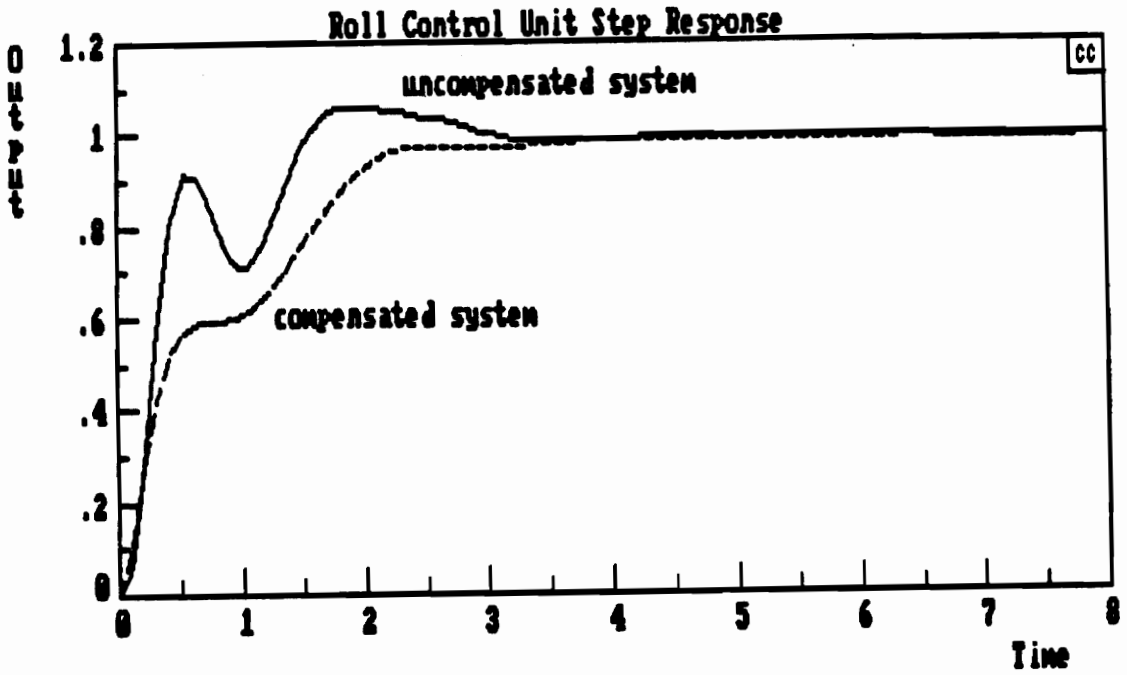


Figure 15: Roll Control Unit Step Response

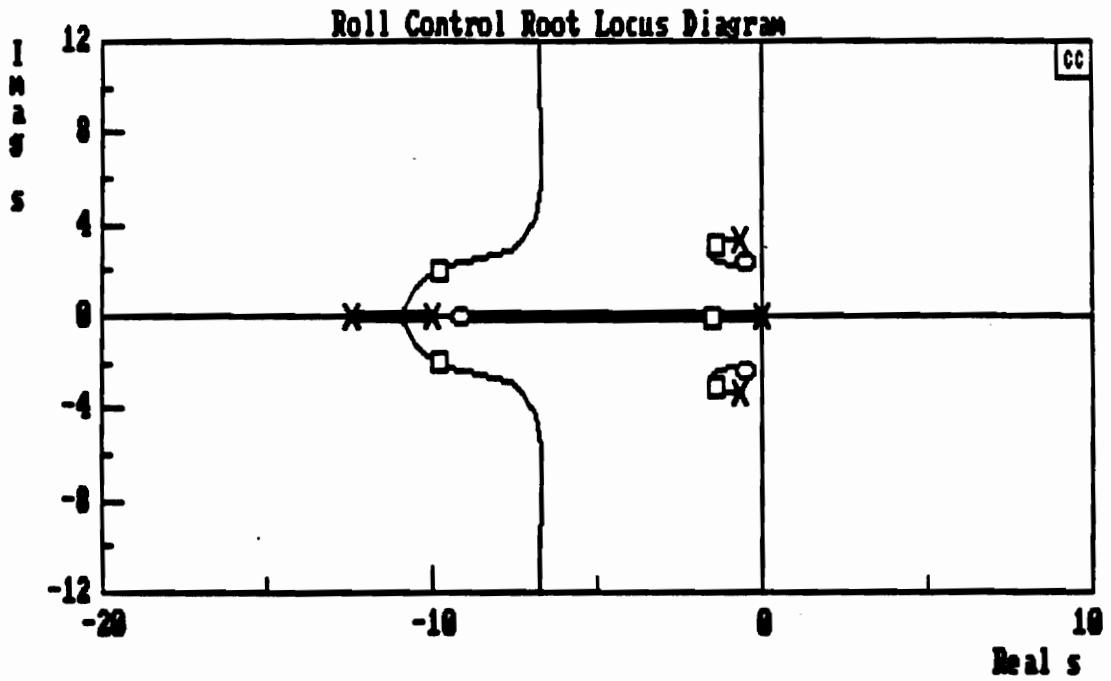


Figure 16: Roll Control Root Locus Diagram

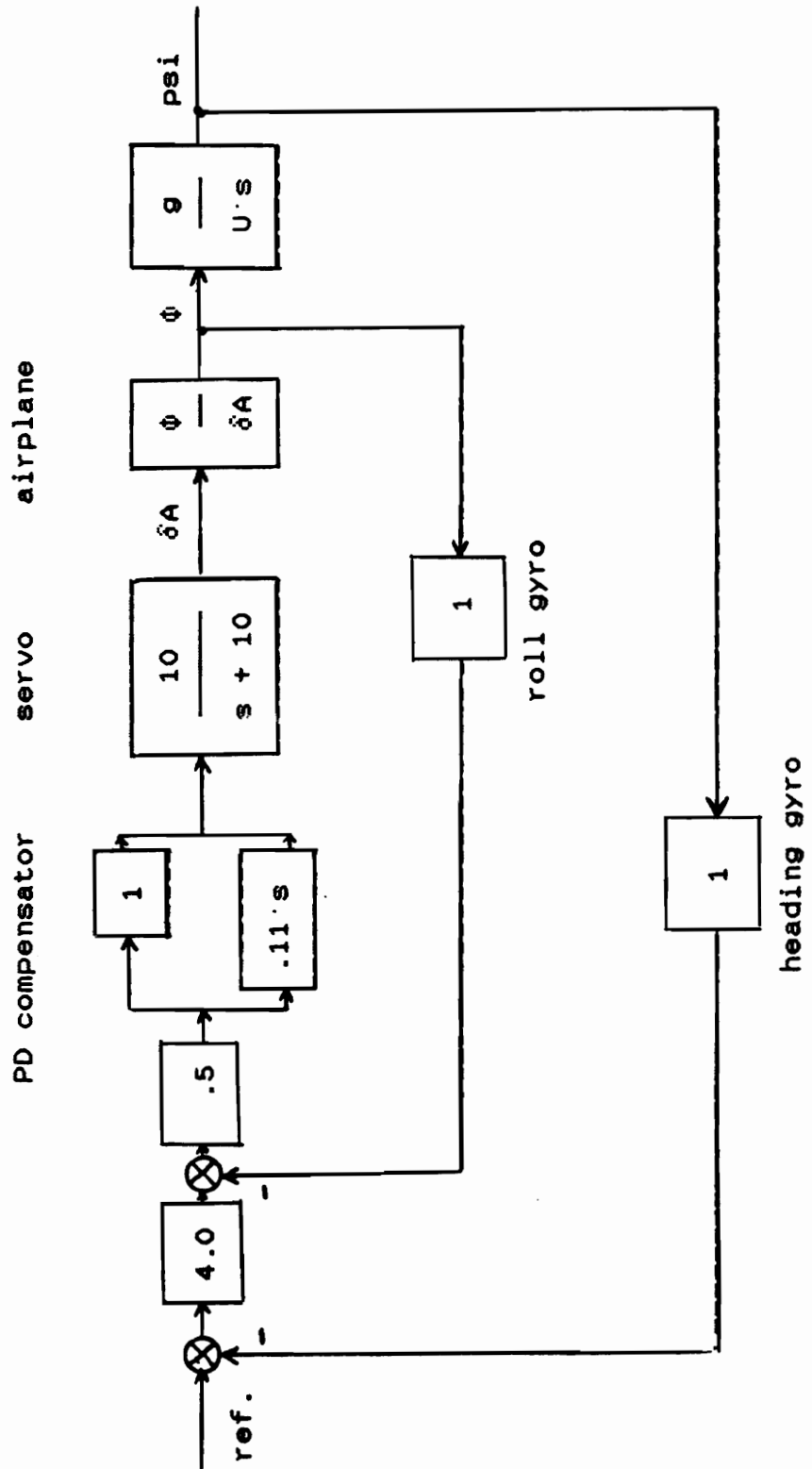


Figure 17: Bank Angle Control and Heading Hold Mode

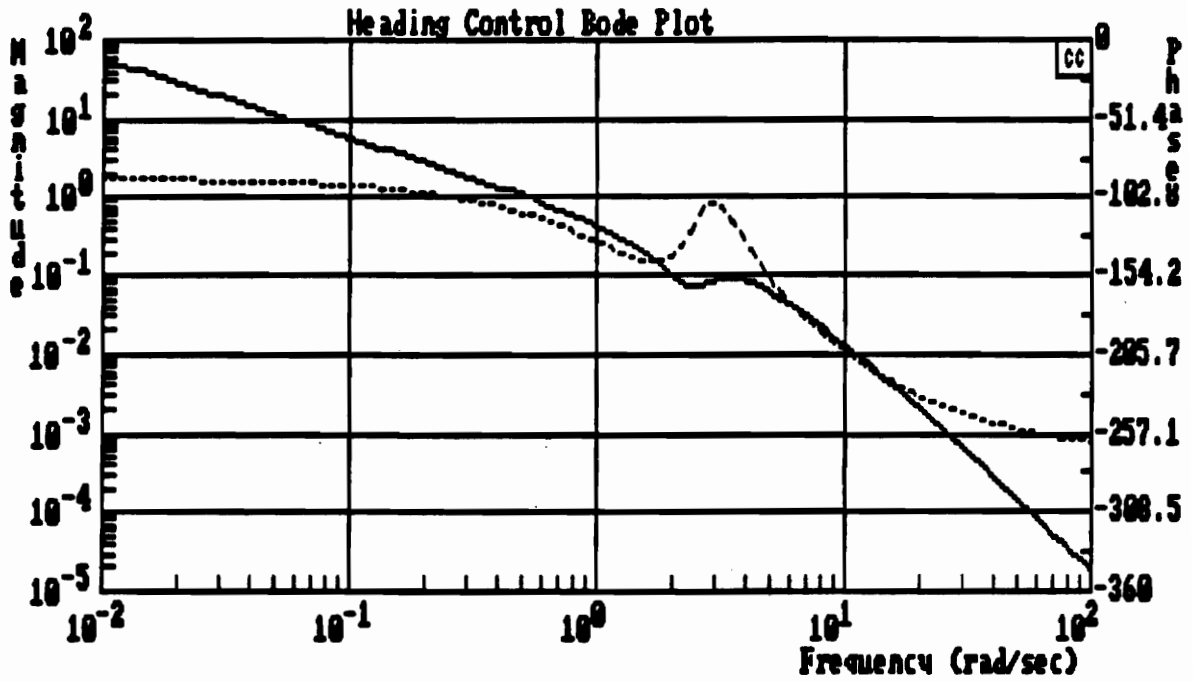


Figure 18: Heading Control Bode Plot

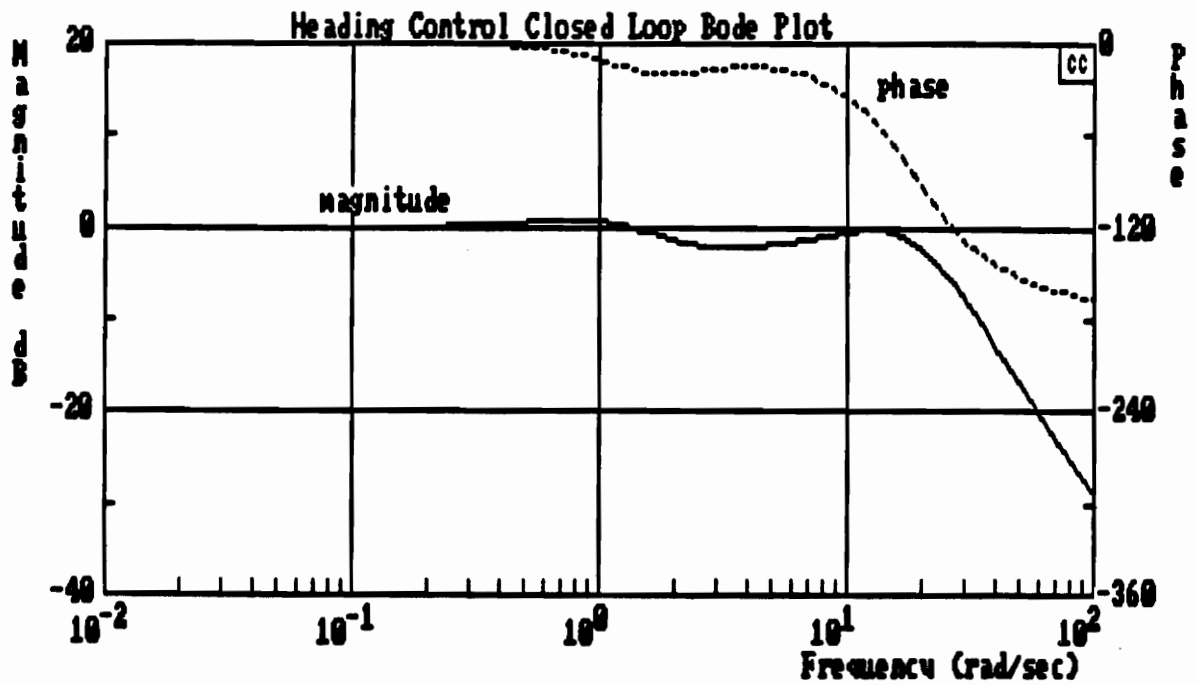


Figure 19: Heading Control Closed Loop Bode Plot

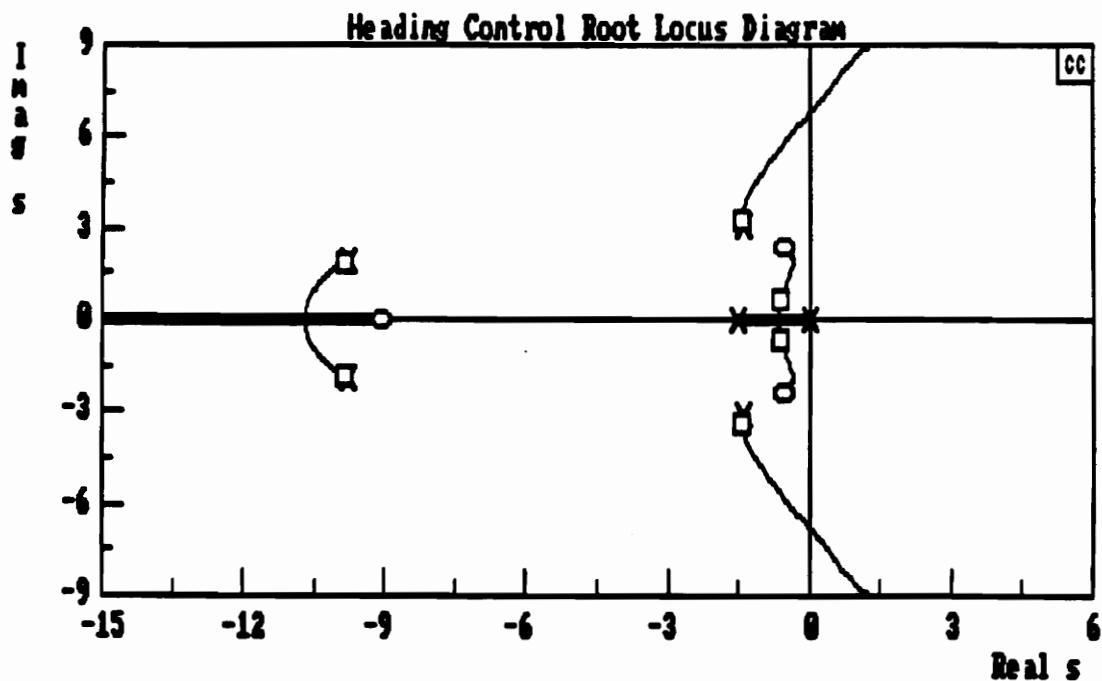


Figure 20: Heading Control Root Locus Diagram

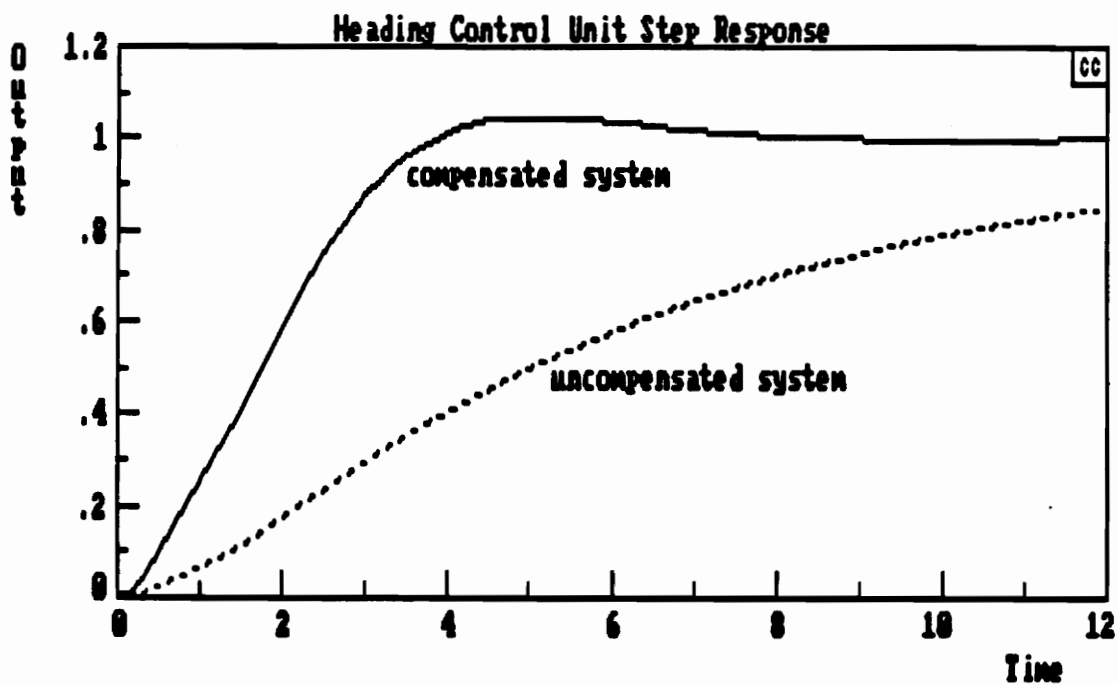


Figure 21: Heading Control Unit Step Response

response curve of the uncompensated system. No additional compensation was needed. All specifications were met by increasing the gain. [2, pg. 1160]

Table 7: Compensator Performance Characteristics

<u>Specification</u>	<u>Control Mode</u>			
	<u>Pitch</u>	<u>Altitude</u>	<u>Roll</u>	<u>Heading</u>
Mp < 1.7 db. (c.l.)	.8	2.2	0	.5
PM > 35 deg.	72	50	75	95
Gain Marg. >9.5 db	30	16	45	26
Phugoid damping	NA	.33	NA	NA
Sh. period damp.	.56	NA	NA	NA
Overshoot < 10%	7%	20%	6%	3%
10-90% rise <3 sec	.5	2	1.8	2.2
SS error < 10%	0	0	.9%	0
Kp > 9	∞	∞	108	∞
Ep < .1	0	0	.009	0
Kv > .1	6.12	.5	0	.59
Ev < 10	.16	2.0	∞	1.68

Chapter 3: IMPLEMENTATION OF CONTROL SYSTEM DESIGN

As described in section 2.3, the roll mode can be accurately approximated using a single degree-of-freedom roll equation. This case was used for part two of the project. The objective of this section was the actual implementation of a feedback control system and compensation circuit. In order to reduce the total moment of inertia about the X axis and make ground testing feasible, a wing section, versus an entire airplane, from a radio control Eagle 63 model airplane was analyzed and the parameters used in the control equations. A squirrel cage ventilation fan provided sufficient air flow to allow testing of the system. The actual hardware used will be described in a later section.

3.1 Simplified Equation of Motion for Single DOF Wing

The equation of motion of an airplane in a single degree of freedom roll is as follows:

$$C_{lda} \delta a(s) Q S B + C_{lp} (\dot{\phi} B) / (2U) Q S B = I_{xx} \ddot{\phi} \quad 3.1$$

The $\phi/\delta a$ transfer function can be determined from this equation and is given in equation 3.2:

$$\phi/\delta a = C_{lda} Q S B / (s^2 I_{xx} - s C_{lp} Q S B / (2U)) \quad 3.2$$

Using dimensional aerodynamic coefficients as defined in Appendix 3, the transfer function is:

$$\phi/\delta a = L_{da} / (s(s + L_p)) \quad 3.3$$

By evaluating the parameters in this equation, the transfer function in the s domain can be determined. [2, pg. 520]

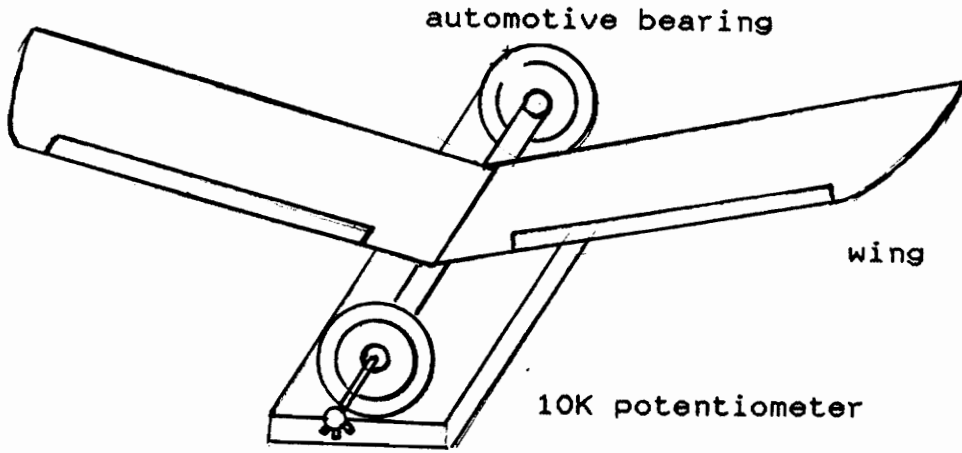
3.2 Test Hardware Description

Figure 22 is a sketch of the experimental system designed to provide a single degree-of-freedom roll axis for the airplane wing. Automotive wheel bearings were pressed onto each end of a threaded shaft. The bearings were then mounted on a 1"x4"x24" board using U-bolts. The shaft was free to rotate parallel to the 24" axis of the board. A fuselage-like structure representing the area immediately below the wing was built for wing attachment. The fuselage-like structure was clamped to the threaded shaft using u-bolts. This structure provided a mounting surface for the wing and allowed a plus or minus 15 degree roll. The wing included the servo which was used in the original model for aileron control.

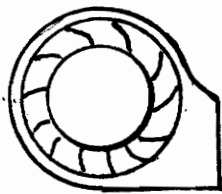
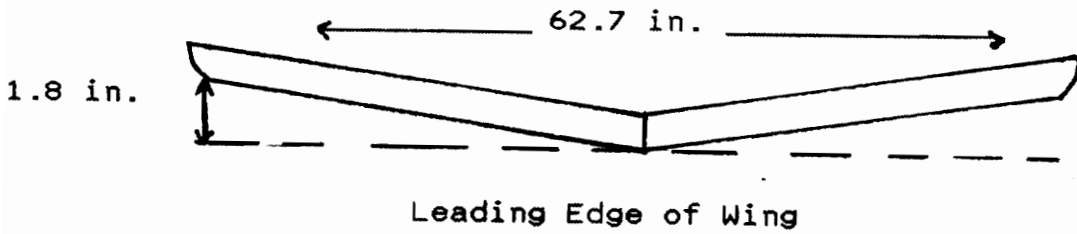
Due to the pulse width modulation design of the receiver/servo system, it was necessary for servo actuation to send all signals into a Futaba four channel Conquest radio. The radio then transmitted the signals to the receiver and into the appropriate channel for servo actuation.

Wing rotation was measured by attaching the body of a 10K ohm potentiometer to the support platform and the rotating arm to the axis of rotation of the threaded shaft. This served as a transducer for converting rotation into an electrical signal.

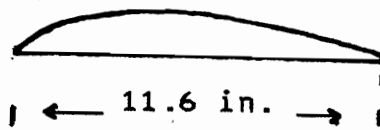
The control circuitry used 761 operational amplifiers in the design of differencing circuits, lead-lag compensators,



Single DOF Roll Platform



Squirrel Cage Fan



Airfoil Section
- constant chord

Figure 22: Experimental Hardware Description

and gain adjustments. Six volt batteries were used to provide a plus or minus bias to the op amps. The supply voltage from the radio was used as the input voltage for the reference and feedback circuits. Figure 23 shows a functional block diagram of the entire system.

Several limitations were inherent in the experimental set-up. Damping was introduced about the roll axis by the bearings and most significantly by the potentiometer. The effect was to slow down system response and remove overshoot that may be introduced by compensator design. Although all control signals were required to be sent through the radio, no model was used to represent these parts of the system. The servo equation used, $10/(s+10)$, is the same equation used in the theoretical part of the project.

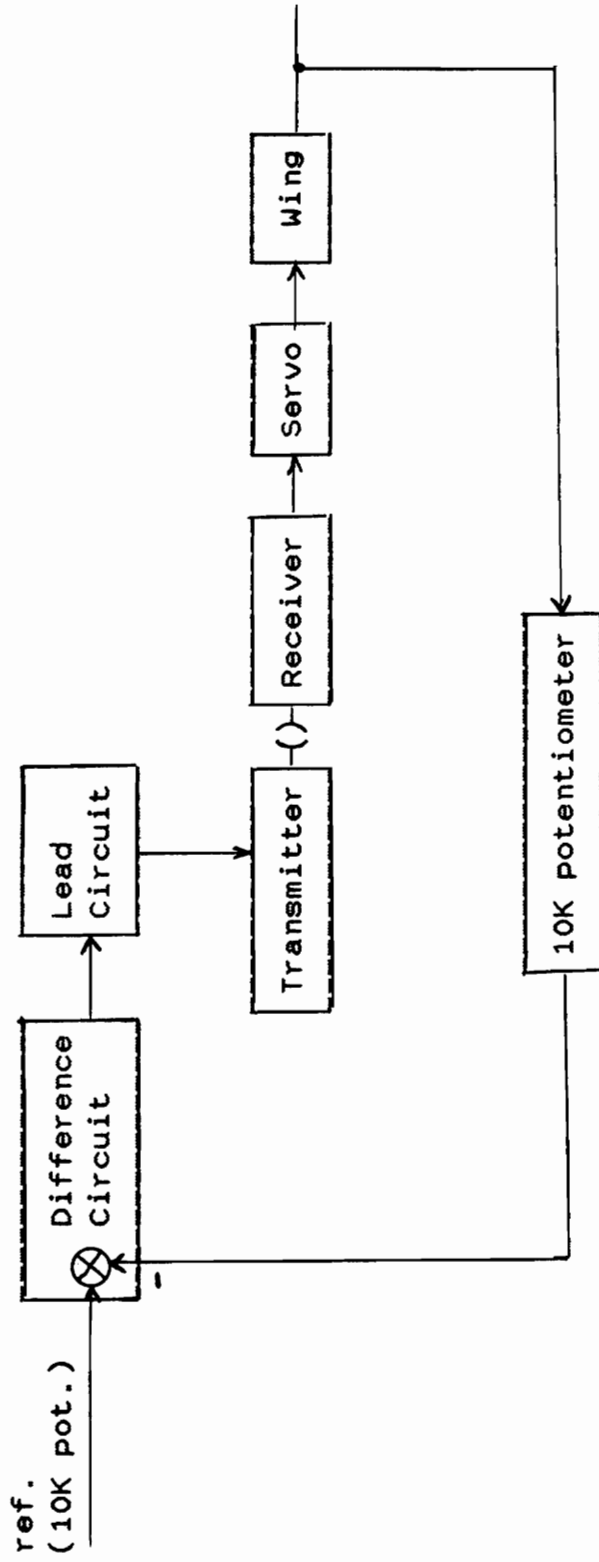


Figure 23: Project Hardware Functional Block Diagram

3.3 Experimental Parameter Determination

3.3.1 Dynamic Pressure - Q

The dynamic pressure of the experimental configuration was determined using the pendulum set-up shown in Figure 24. A tennis ball was hung from a 2 foot string and the amount of deflection resulting from the fan pressure measured. The force balance equations are shown in Figure 24.

The deflection of the tennis ball was measured across the leading edge of the wing. The average deflection was 5 inches. Given the weight and diameter of the tennis ball (2 oz. and 2.5 in.) and length of string (2 ft.), the pressure was determined to be .76 lb/ft.².

3.3.2 Forward Velocity - U

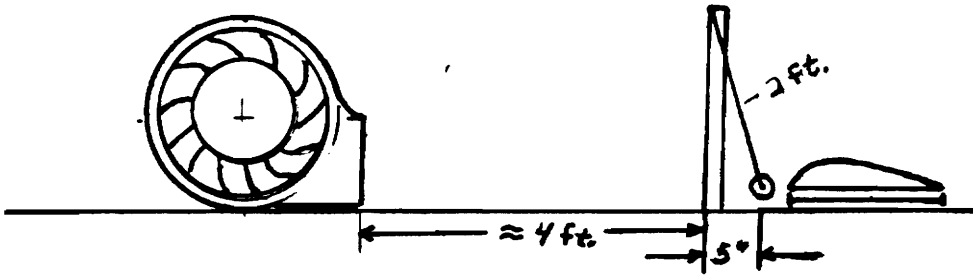
The forward velocity is related to dynamic pressure by equation:

$$q = C_d * 1/2 \rho * \text{Velocity}^2 \quad 3.4$$

where C_d is the drag coefficient and ρ is the air density which is equal to .002378 lb sec²/ft⁴ at sea level. C_d for a sphere is given as .5. [7, pg. 430] From the previous value of q , the velocity is found to be 36.1 ft/sec. or 24.6 miles/hr.

3.3.3 Wing Area - S

From the manufacturer's specifications, the wing area is



Fan

Pendulum

Wing

$$\text{Tennis ball mass: } mg := \frac{2}{16} \text{ lbs force}$$

$$\text{Tennis ball diameter: } d := \frac{2.5}{12} \text{ ft.}$$

$$\text{Projected area: } a := \pi \frac{d^2}{4} \quad a = 0.034$$

$$\text{Force in x direct. } F_x := mg \sin(\theta) \quad F_x = 0.026$$

$$\text{Dynamic Pressure: } q := \frac{F_x}{a} \quad q = 0.764$$

$$\text{Air Density: } \rho := .002378 \text{ lbs.} \cdot \text{sec.}^2 / \text{ft.}^4$$

$$\text{Drag Coefficient: } C_d := .5$$

Air Velocity:

$$V := \sqrt{\frac{q}{.5 \cdot \rho \cdot C_d}} \quad V = 35.847 \text{ ft./sec.}$$

Figure 24: Dynamic Pressure Calculation

given as 4.96 ft^2 .

3.3.4 Wing Span - B

The manufacturer specifies the wing span as 62.7 inches which equals 5.2 ft.

3.3.5 Wing Moment of Inertia - I_{xx}

The total wing weight is 11 oz. The equation for moment of inertia is given by:

$$I_{xx} = 1/12*(m*l^2) \quad 3.5$$

I_{xx} is found to be 1.52 lb ft^2 . In the experimental configuration, additional moment of inertia is added by the platform to support the wing. This weight was very close to the x axis so no attempt was made to add this additional inertia.

3.3.6 Aerodynamic Coefficients - (C_{lda} , C_p , L_{da} , L_p)

The nondimensional aerodynamic coefficients, C_{lda} and C_p , are given for this particular class of flight in reference 2, chapter 4, as follows: $C_{lda} = .15$ and $C_{lp} = -.40$.

From these values and the above determined parameters, the dimensional coefficients can be found and the transfer function for the wing experiment determined. L_{da} and L_p are given by equations 3.6 and 3.7:

$$L_{da} = q*s*b*C_{lda}/(I_{xx}) \quad 3.6$$

$$L_p = q*s*b^2*C_{lp}/(2*I_{xx}*U) \quad 3.7$$

Substituting into these equations, $L_{da} = 1.92$ and $L_p = -.52$.

The transfer function given earlier in equation 3.3 is then:

$$\phi/da = 1.92/(s*(s+.37)) \quad 3.8$$

3.4 Project Performance Specifications

Performance specifications for the project are equivalent to those in section 2.3.

- Frequency Response;
- $M_p < 1.7$ db. for dominant mode
 - Phase Margin > 35 degrees
 - Gain Margin > 9.5 db
 - Damping (phugoid) $> .04$
 - Damping (short period) $.30 < D_{sp} < 2.0$
- Time Domain;
- Overshoot $< 10\%$
 - Rise Time (10% to 90%) < 3 sec.
 - Steady State Error $< 10\%$
- Error Specifications;
- $K_p > 9$, $E_p < .1$
 - $K_v > .1$, $E_v < 10$

3.5 Compensator Design

The desired performance of the system is to have a natural frequency of 2.5 rad/sec. and damping of .7. This means the dominant closed loop poles in the denominator will have the equation:

$$(s^2 + 2*2.5*.7*s + 2.5^2) \quad 3.9$$

The servo equation used was $10/(s+10)$ and the open loop transfer function of the system is:

$$10/(s+10)*.0722/(s*(s+.09)) \quad 3.10$$

A Bode plot of the transfer function indicates that a phase lead circuit is desired to improve phase margin and gain margin. The compensation design options were limited to a simple lead or lag circuit since the compensator would be implemented in electronic hardware; however, the roll equation is already in the form of a type 1 system. Figures 25 through 29 include the system response diagrams. From the root locus diagram of the system, a phase lead compensator of $(s+.5)/(s+5)$ was chosen to allow a root locus which would provide options for closed loop poles close to the desired values stated in equation 9.1. With the gain at $k=4$, the closed loop poles are shown in the diagram. These poles result in a natural frequency of 2.48 rad/sec. and a damping value of .69. Figure 30 shows a block diagram of the system design. From the Bode diagrams, the closed loop peak magnitude response is 0 db.; the gain margin is 20 db., and

the phase margin is 65 degrees. The 10% to 90% rise time is 1 sec., and the steady state error is zero. The velocity error coefficient is $K_v=2.07$, and the steady state velocity error is .48. The control system meets all specified requirements.

Implementation of the compensation circuit can be achieved using op amp circuit designs shown in Figure 31. [8, chp. 8] and [9, chp. 4] Prior to compensation, a feedback circuit must be established and compared to a reference input. This error signal is then sent into the compensation circuit. The gain of the circuit is determined by the pole and zero locations and the scaling of the resistor and capacitor values. [9, App. 1] Another op amp circuit is used to adjust the gain to the desired value. The resistor and capacitor values used to build the circuit are shown below:

<u>Difference Circuit</u>	<u>Lead Circuit</u>	<u>Gain Circuit</u>
R1 = 10k pot.	R5 = 105k ohms	R7 = 58.3k ohms
R2 = 10k pot.	R6 = 1.01m ohms	R8 = 85.1k ohms
R3 = 5.9k ohms	C1 = .1 micro farads	
R4 = 6.1k ohms		

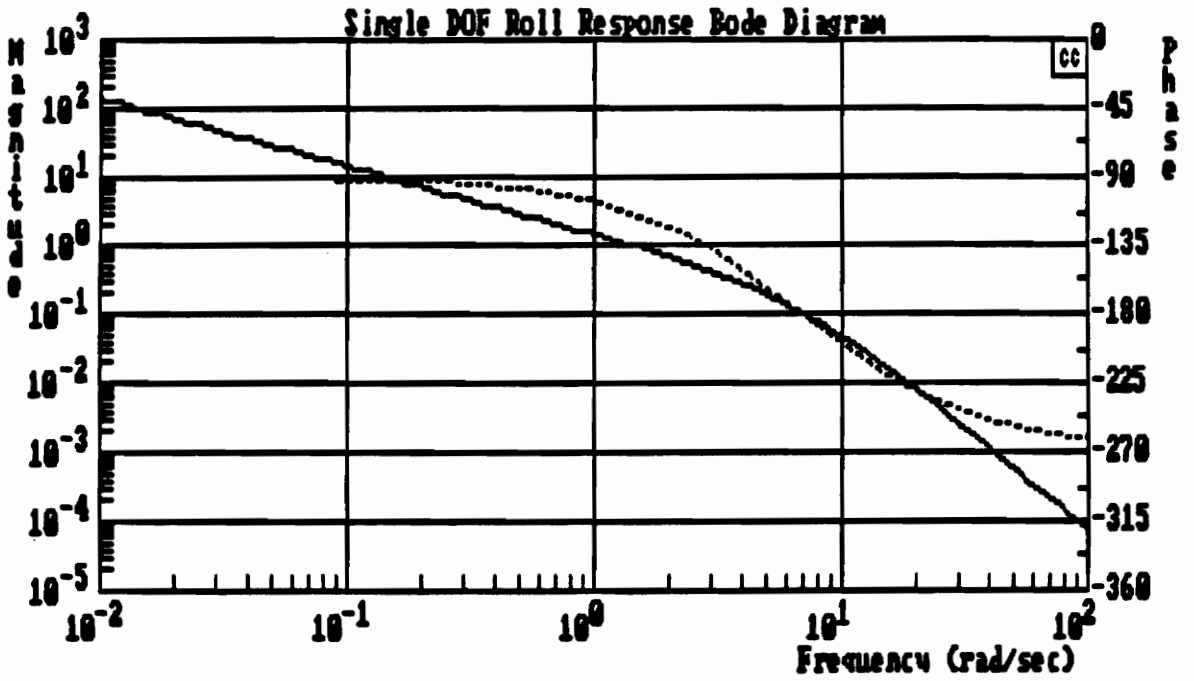


Figure 25: Single DOF Roll Response Bode Diagram

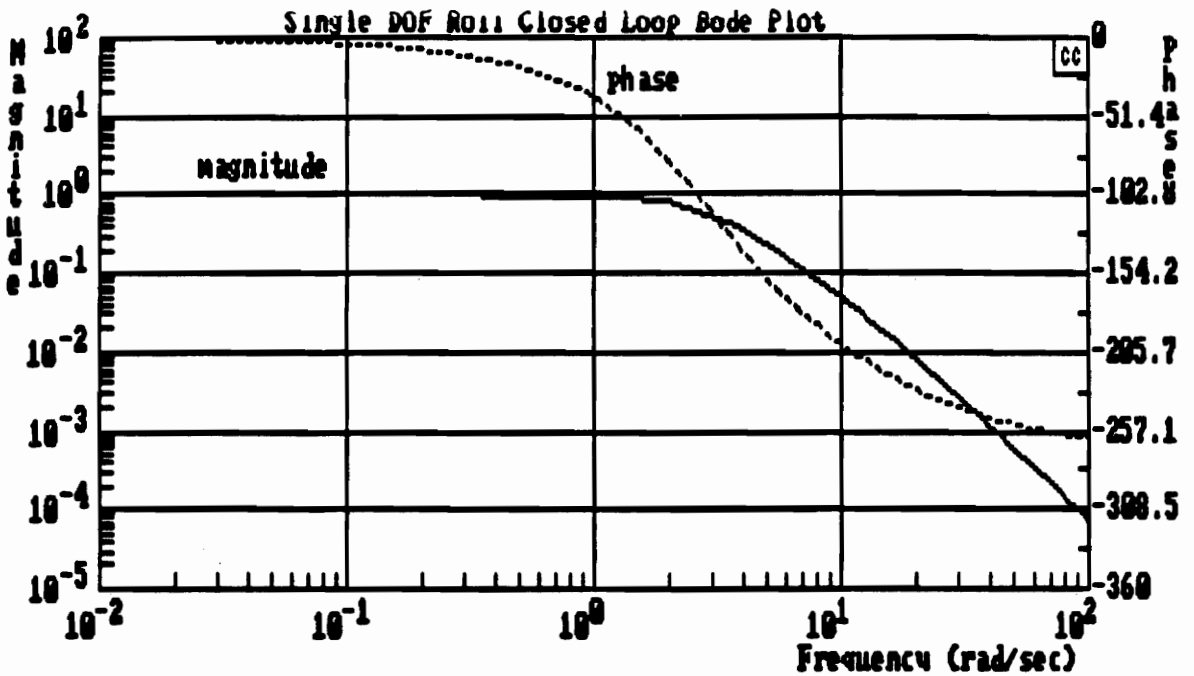


Figure 26: Single DOF Roll Closed Loop Bode Plot

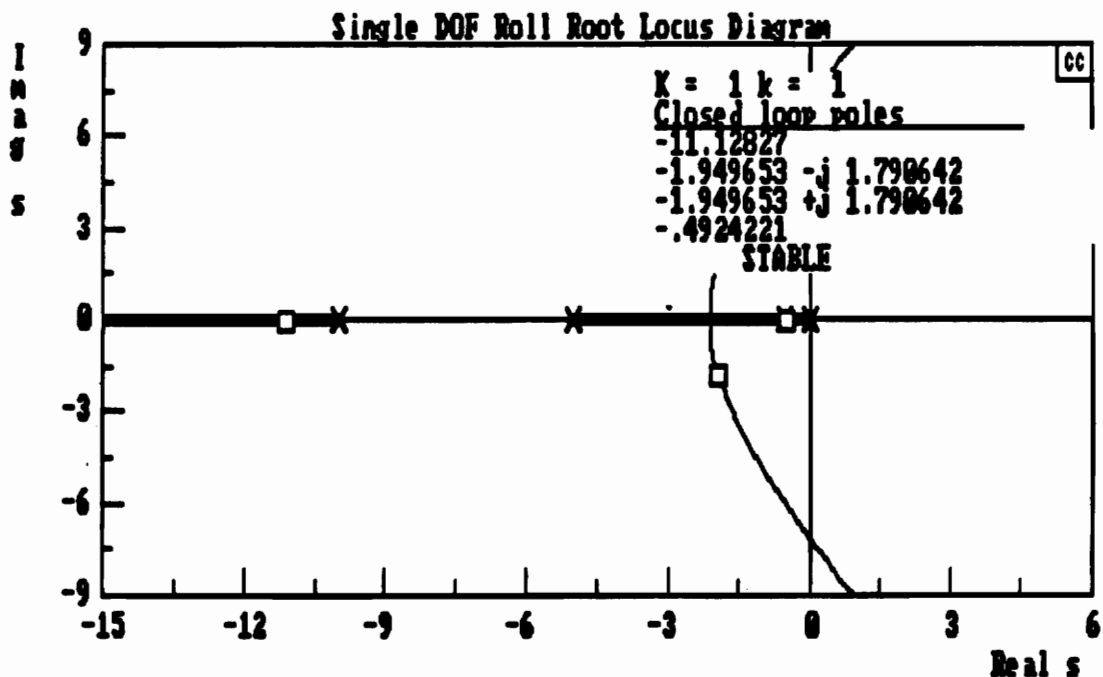


Figure 27: Single DOF Roll Root Locus Diagram

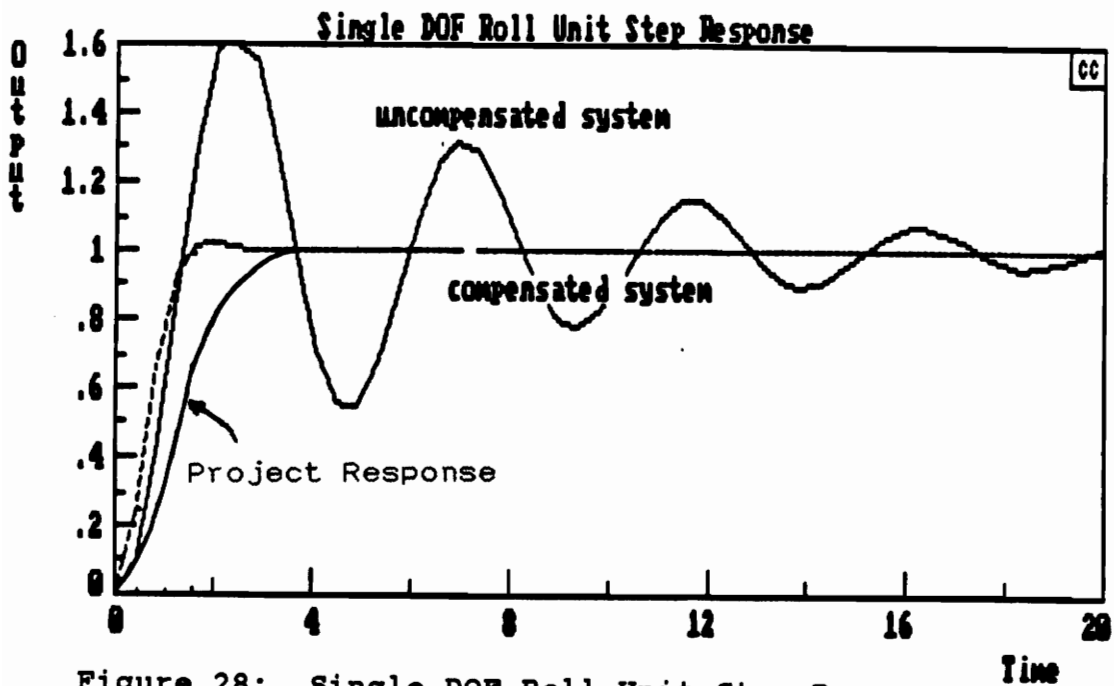


Figure 28: Single DOF Roll Unit Step Response

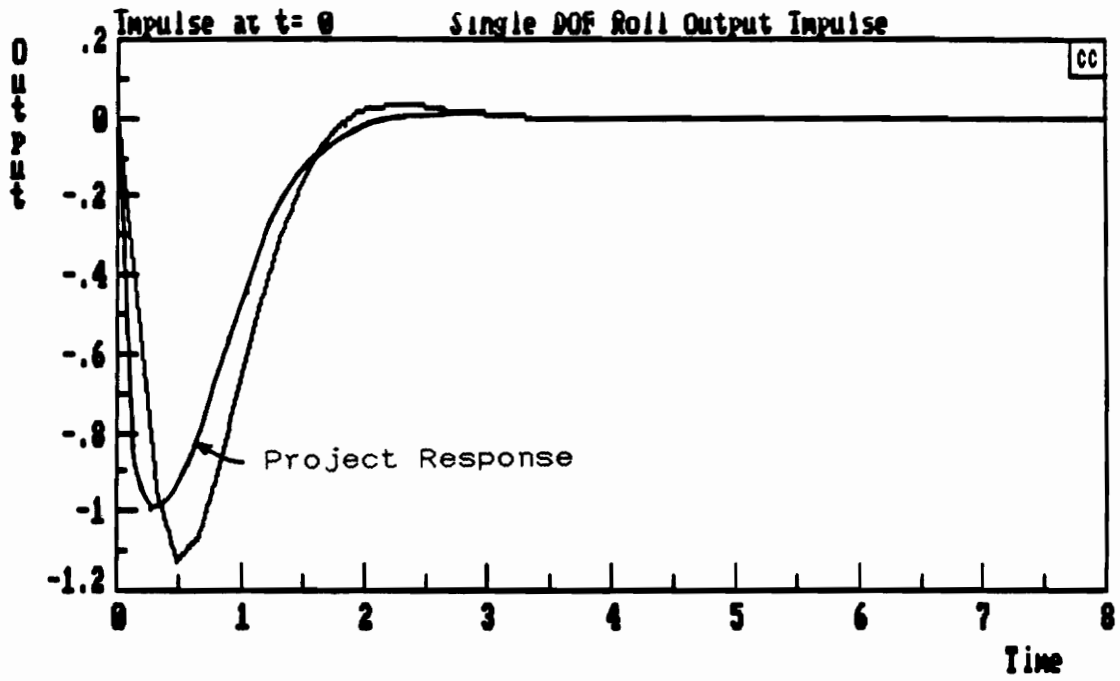


Figure 29: Single DOF Roll Output Impulse Response

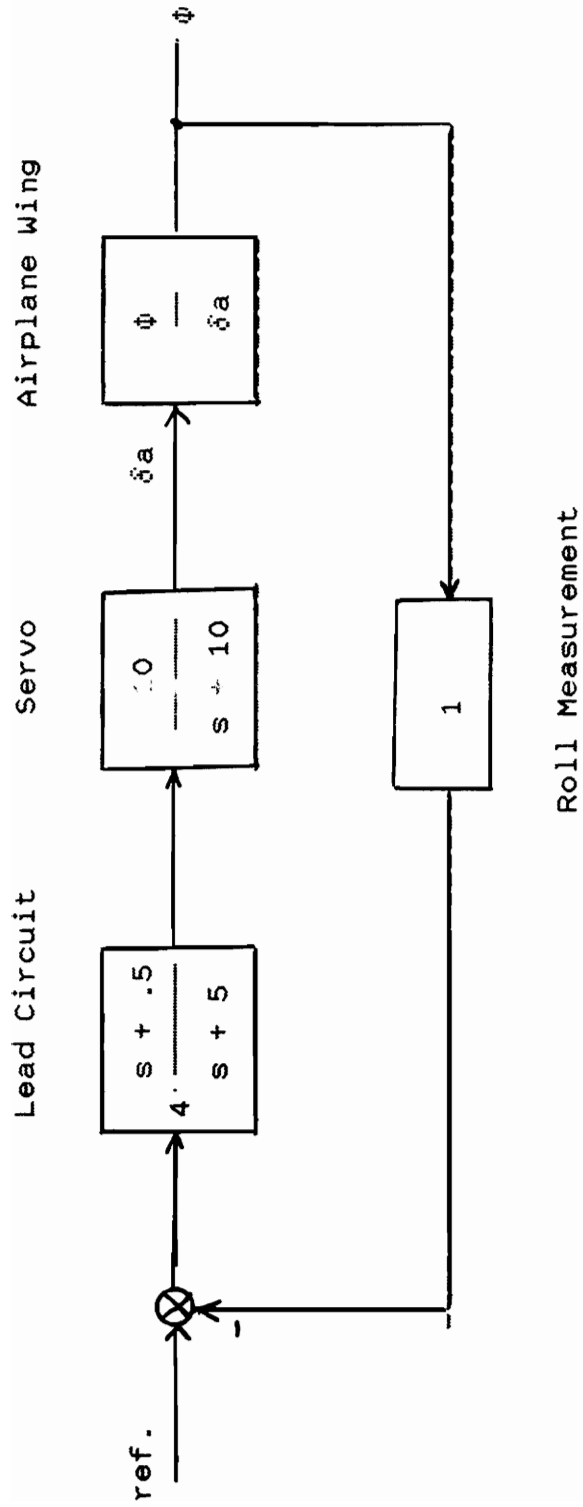
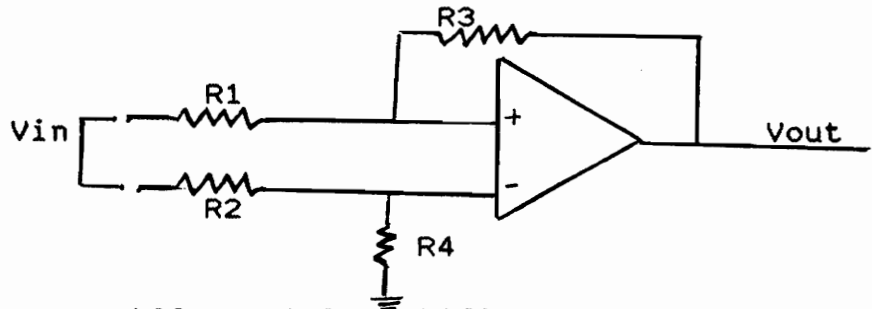


Figure 30: Single DOF Roll Control

$$k := \frac{R3}{R1}$$

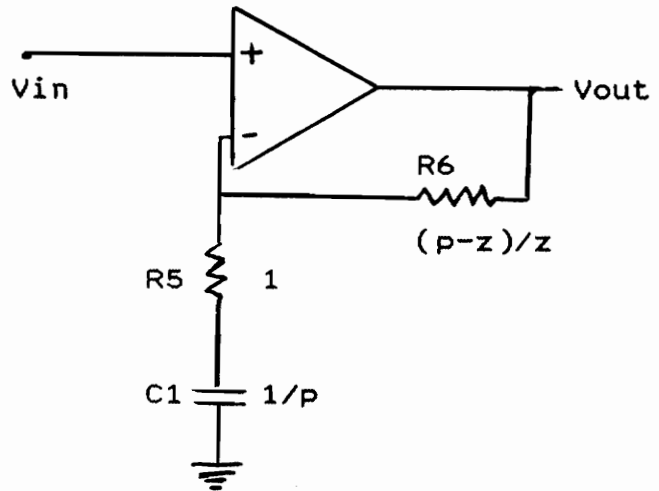


Differential Amplifier

$$\text{lead: } K \cdot \frac{s + z}{s + p}$$

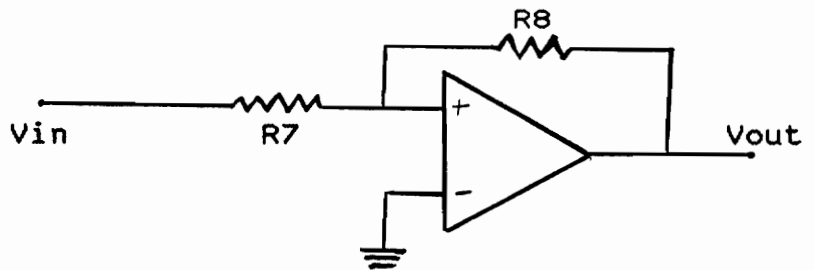
$$p > z$$

$$K := \frac{p}{z}$$



Lead Circuit Design

$$K := \frac{R7}{R8}$$



Gain Circuit Design

Figure 31: Operational Amplifier Circuit Design

3.6 System Test Results

Testing of the system was accomplished using a video camera. The tests consisted of applying step inputs to the system by adjusting the value of the reference potentiometer, and creating a disturbance by rapping one end of the wing and watching the response. Figures 28 and 29 include the response of the system. The test results are not fully representative of the an actual system due to increased damping in the set-up, some uncertainty in the experimental parameters, the pulse width modulation design of the radio and receiver, and limited resolution of the measuring system. However, the results do indicate that the airplane wing response meets the time response specifications.

Chapter 4: SUMMARY AND CONCLUSIONS

4.1 Project Conclusions

The results of part 1 demonstrated the determination of airplane transfer functions and applied these to a specific airplane geometry and flight condition. Given the transfer functions, several autopilot control systems were designed to meet performance specifications. The design method of using a PID controller provided the desired frequency loop shaping and the steady state response to a step input.

Part two used a simplified single degree-of-freedom roll model and implemented a control system design. The system performed close to theoretical calculations. A more accurate measurement system would be required to obtain actual performance. There was some uncertainty in the aerodynamic coefficients used for the flight condition, and the experimental set-up introduced additional damping and inertias. However, the performance achieved was representative of actual flight conditions.

The objectives of this project were successfully accomplished. As a result, the project demonstrated the feasibility of designing, implementing, and testing in a simulated environment an automatic flight control system. These control system designs can be applied to flight autopilot hardware.

4.2 Suggestions for Further Study

During completion of the project, several additional study topics surfaced. One is to consider simultaneously controlling several airplane modes. This might require multiple inputs to a single control surface. An optimum performance measure would have to be determined and a control system algorithm developed for control surface deflection. Also, the designs described in this project did not take into account the equations of the control surfaces and their mechanisms. A complete control system design would have to consider the forces required to actuate the surfaces. Finally, additional complexity could be added to the implementation part of the project by using a rate gyro. Since the system is second order, this would provide state variable feedback and allow arbitrary placement of zeros to obtain desired damping and frequency characteristics.

REFERENCES

1. Etkin, Bernard., Dynamics of Atmospheric Flight. New York: John Wiley and Sons, 1972.
2. Roskam, Jan., Airplane Flight Dynamics and Automatic Flight Controls. Lawrence, KS: Roskam Aviation and Engineering Corporation, 1979.
3. Perkins, Courtland D. and Hage, Robert E., Airplane Performance Stability and Control. New York: John Wiley and Sons, 1949.
4. Etkin, Bernard., Dynamics of Flight. New York: John Wiley and Sons, 1959.
5. Thompson, Peter M., "Program CC". Hawthorne, CA: Systems Technology Inc., 1988
6. Takahashi, Yasundo; Michael J. Rabins; and David M. Auslander., Control. Reading, MA: Addison-Wesley Publishing, 1970.
7. Roberson, John A., Crowe, Clayton T., Engineering Fluid Mechanics. Boston, MA: Houghton Mifflin Co., 1980
8. Horn, Delton, T., Amplifiers Simplified. Blue Ridge Summit, PA: Tab Books, 1987.
9. Van Valkenburg, M. E., Analog Filter Design. New York, NY: CBS College Publishing, 1982.

Appendix 1: Example Airplane Flight Condition
and Geometries

Flight Condition:

Altitude (ft)	$h := 5000$
Air Density (slugs/ft ³)	$\rho := .00205$
Speed (fps)	$U1 := 219$
Center of Gravity	$x_{cg} := .25$
Initial Attitude (θ in rad)	$\theta := 0$
Dynamic Pressure (lbs/ft ²)	$q := 49.19$

Geometry and Inertias:

Wing area (ft ²)	$s := 174$
Wing Span (ft)	$b := 35.8$
Wing Mean Geometric Chord (ft)	$c := 4.9$
Weight (lbsm)	$w := 82.14$
I_{xx} (slug ft ² , lb ft ²)	$I_{xx} := 948$
I_{yy} (slug ft ² , lb ft ²)	$I_{yy} := 1346$
I_{zz} (slug ft ² , lb ft ²)	$I_{zz} := 1967$
I_{xz} (slug ft ² , lb ft ²)	$I_{xz} := 0$

Steady State Coefficients:

$CL1 := .31$	$CTX1 := .031$	$CMT1 := 0$
$CD1 := .031$	$CM1 := 0$	

Appendix 2: Longitudinal Transfer Functions
 from Stability and Control Derivatives

Nondimensional Longitudinal Derivatives

CMU := 0	CLA := 4.6	CDDE := .06
CMA := -.89	CLAD := 1.7	CMDE := -1.28
CMAD := -5.2	CLQ := 3.9	
CMQ := -12.4	CDA := .13	
CMTU := 0	CDU := 0	
CMTA := 0	CTXU := -.093	
CLU := 0	CLDE := .43	

Dimensional Longitudinal Stability Derivatives

$XU := -q \cdot s \cdot \frac{CDU + 2 \cdot CD1}{w \cdot U1}$	$XTU := q \cdot s \cdot \frac{CTXU + 2 \cdot CTX1}{w \cdot U1}$
$XA := -q \cdot s \cdot \frac{CDA - CL1}{w}$	$XDE := -q \cdot s \cdot \frac{CDDE}{w}$
$ZU := -q \cdot s \cdot \frac{CLU + 2 \cdot CL1}{w \cdot U1}$	$ZA := -q \cdot s \cdot \frac{CLA + CD1}{w}$
$ZAD := -q \cdot s \cdot CLAD \cdot \frac{c}{2 \cdot w \cdot U1}$	$ZQ := -q \cdot s \cdot CLQ \cdot \frac{c}{2 \cdot w \cdot U1}$

Appendix 2 (cont.): Longitudinal Transfer Functions

$$ZDE := -q \cdot s \cdot c \cdot \frac{CLDE}{w}$$

$$MU := q \cdot s \cdot c \cdot \frac{CMU + 2 \cdot CM1}{I_{yy} \cdot U1}$$

$$MTU := q \cdot s \cdot c \cdot \frac{CMTU + 2 \cdot CMT1}{I_{yy} \cdot U1}$$

$$MA := q \cdot s \cdot c \cdot \frac{CMA}{I_{yy}}$$

$$MTA := q \cdot s \cdot c \cdot \frac{CMTA}{I_{yy}}$$

$$MAD := q \cdot s \cdot c \cdot \frac{2 \cdot CMAD}{2 \cdot I_{yy} \cdot U1}$$

$$MQ := q \cdot s \cdot c \cdot \frac{2 \cdot CMQ}{2 \cdot I_{yy} \cdot U1}$$

$$MDE := q \cdot s \cdot c \cdot \frac{CMDE}{I_{yy}}$$

$$XU = -0.029$$

$$MDE = -39.883$$

$$XTU = -0.015$$

$$MQ = -4.322$$

$$XA = 18.756$$

$$MAD = -1.813$$

$$XDE = -6.252$$

$$MTA = 0$$

$$ZU = -0.295$$

$$MA = -27.731$$

$$ZA = -482.554$$

$$MTU = 0$$

$$ZAD = -1.982$$

$$MU = 0$$

$$ZQ = -4.546$$

$$ZDE = -44.806$$

Appendix 2 (cont.): Longitudinal Transfer Functions

Denominator Polynomial

$$AD1 := U1 - ZAD$$

$$BD1 := -(U1 - ZAD) \cdot (XU + XTU + MQ) - ZA - MAD \cdot (U1 + ZQ)$$

$$CD11 := (XU + XTU) \cdot (MQ \cdot (U1 - ZAD) + ZA + MAD \cdot (U1 + ZQ))$$

$$CD12 := MQ \cdot ZA - ZU \cdot XA + MAD \cdot g \cdot \sin(\theta) - (MA + MTA) \cdot (U1 + ZQ)$$

$$CD1 := CD11 + CD12$$

$$DD11 := g \cdot \sin(\theta) \cdot (MA + MTA - MAD \cdot (XU + XTU))$$

$$DD12 := g \cdot \cos(\theta) \cdot (ZU \cdot MAD + (MU + MTU) \cdot (U1 - ZAD))$$

$$DD13 := (MU + MTU) \cdot (-XA \cdot (U1 + ZQ))$$

$$DD14 := ZU \cdot XA \cdot MQ + (XU + XTU) \cdot ((MA + MTA) \cdot (U1 + ZQ) - MQ \cdot ZA)$$

$$DD1 := DD11 + DD12 + DD13 + DD14$$

$$ED11 := g \cdot \cos(\theta) \cdot ((MA + MTU) \cdot ZU - ZA \cdot (MU + MTU))$$

$$ED12 := g \cdot \sin(\theta) \cdot ((MU + MTU) \cdot XA - (XU + XTU) \cdot (MA + MTA))$$

$$ED1 := ED11 + ED12$$

$$AD1 = 220.982$$

3

$$DD1 = 396.583$$

$$CD1 = 8.119 \cdot 10$$

3

$$BD1 = 1.836 \cdot 10$$

$$ED1 = 263.416$$

The denominator polynomial is given by the following:

$$f(s) := AD1 \cdot s^4 + BD1 \cdot s^3 + CD1 \cdot s^2 + DD1 \cdot s + ED1$$

Appendix 2 (cont.): Longitudinal Transfer Functions

Roots of denominator:

guess value	solve command	solution for s
$s := 1 + i$	$s := \text{root}(f(s),s)$	$s = -0.021 + 0.18i$
$s := 1 - i$	$s := \text{root}(f(s),s)$	$s = -0.021 - 0.18i$
$s := -10 - 10i$	$s := \text{root}(f(s),s)$	$s = -4.134 - 4.39i$
$s := -10 + 10i$	$s := \text{root}(f(s),s)$	$s = -4.134 + 4.39i$

Numerator for $U/\delta E$ Transfer Function

$$AU := XDE \cdot (U1 - ZAD)$$

$$BU := -XDE \cdot ((U1 - ZAD) \cdot MQ + ZA + MAD \cdot (U1 + ZQ)) + ZDE \cdot XA$$

$$CU1 := XDE \cdot (MQ \cdot ZA + MAD \cdot g \cdot \sin(\theta) - (MA + MTA) \cdot (U1 + ZQ))$$

$$CU2 := ZDE \cdot (-MAD \cdot g \cdot \cos(\theta) - XA \cdot MQ)$$

$$CU3 := MDE \cdot (XA \cdot (U1 + ZQ) - (U1 - ZAD) \cdot g \cdot \cos(\theta))$$

$$CU := CU1 + CU2 + CU3$$

$$DU1 := XDE \cdot (MA + MTA) \cdot g \cdot \sin(\theta) - ZDE \cdot MA \cdot g \cdot \cos(\theta)$$

$$DU2 := MDE \cdot (ZA \cdot g \cdot \cos(\theta) - XA \cdot g \cdot \sin(\theta))$$

$$DU := DU1 + DU2$$

$$AU = -1.382 \cdot 10^3$$

$$CU = 6.69 \cdot 10^4$$

$$BU = -1.226 \cdot 10^4$$

$$DU = 5.797 \cdot 10^5$$

Appendix 2 (cont.): Longitudinal Transfer Functions

$$f(s) := AU \cdot s^3 + BU \cdot s^2 + CU \cdot s + DU$$

$$s := -5 \qquad s := \text{root}(f(s), s) \qquad s = -6.628$$

$$s := 0 \qquad s := \text{root}(f(s), s) \qquad s = -9.158$$

$$s := 20 \qquad s := \text{root}(f(s), s) \qquad s = 6.913$$

Numerator for $\alpha/\delta E$ transfer function

$$AA := ZDE$$

$$BA := XDE \cdot ZU + ZDE \cdot (-MQ - (XU + XTU)) + MDE \cdot (U1 + ZQ)$$

$$CA1 := XDE \cdot ((U1 + ZQ) \cdot (MU + MTU) - MQ \cdot ZU)$$

$$CA2 := ZDE \cdot MQ \cdot (XU + XTU)$$

$$CA3 := MDE \cdot (-g \cdot \sin(\theta) - (U1 + ZQ) \cdot (XU + XTU))$$

$$CA := CA1 + CA2 + CA3$$

$$DA1 := -XDE \cdot (MU + MTU) \cdot g \cdot \sin(\theta) + ZDE \cdot (MU + MTU) \cdot g \cdot \cos(\theta)$$

$$DA2 := MDE \cdot ((XU + XTU) \cdot g \cdot \sin(\theta) - ZU \cdot g \cdot \cos(\theta))$$

$$DA := DA1 + DA2$$

$$AA = -44.806$$

$$CA = -379.067$$

$$BA = -8.747 \cdot 10^3$$

$$DA = -378.845$$

$$f(s) := AA \cdot s^3 + BA \cdot s^2 + CA \cdot s + DA$$

Appendix 2 (cont.): Longitudinal Transfer Functions

```

s := -1 - i          s := root(f(s),s)      s = -0.022 - 0.207i
s := -1 + i          s := root(f(s),s)      s = -0.022 + 0.207i
s := -195            s := root(f(s),s)      s = -195.171

```

Numerator for $\theta/\delta E$ transfer function
$$A_{\theta} := ZDE \cdot MAD + MDE \cdot (U1 - ZAD)$$

$$B_{\theta 1} := XDE \cdot (ZU \cdot MAD + (U1 - ZAD) \cdot (MU + MTU))$$

$$B_{\theta 2} := ZDE \cdot ((MA + MTA) - MAD \cdot (XU + XTU))$$

$$B_{\theta 3} := MDE \cdot (-ZA - (U1 - ZAD) \cdot (XU + XTU))$$

$$B_{\theta} := B_{\theta 1} + B_{\theta 2} + B_{\theta 3}$$

$$C_{\theta 1} := XDE \cdot ((MA + MTA) \cdot ZU - ZA \cdot (MU + MTU))$$

$$C_{\theta 2} := ZDE \cdot (-(MA + MTA) \cdot (XU + XTU) + XA \cdot (MU + MTU))$$

$$C_{\theta 3} := MDE \cdot (ZA \cdot (XU + XTU) - XA \cdot ZU)$$

$$C_{\theta} := C_{\theta 1} + C_{\theta 2} + C_{\theta 3}$$

$$A_{\theta} = -8.732 \cdot 10^3 \qquad B_{\theta} = -1.839 \cdot 10^4 \qquad C_{\theta} = -1.068 \cdot 10^3$$

$$f(s) := A_{\theta} \cdot s^2 + B_{\theta} \cdot s + C_{\theta}$$

```

s := -1          s := root(f(s),s)      s = -0.06
s := -2          s := root(f(s),s)      s = -2.047

```

Appendix 3: Lateral Transfer Functions form Stability
and Control Derivatives

Nondimensional Lateral Derivatives

CLP := -.47	CLB := -.089
CLDA := .178	CLR := .096
CLDR := .0147	CNB := .065
CNDA := -.053	CNP := -.03
CNDR := -.0657	CNR := -.099
CYB := -.31	CYP := -.037
CYDR := .187	CYR := .21
CNTB := 0	CYDA := 0

Dimensional Lateral Stability Derivatives

$$YB := q \cdot s \cdot \frac{CYB}{w}$$
$$YP := q \cdot s \cdot b \cdot \frac{CYP}{2 \cdot w \cdot U1}$$
$$YR := q \cdot s \cdot b \cdot \frac{CYR}{2 \cdot w \cdot U1}$$
$$YDA := q \cdot s \cdot \frac{CYDA}{w}$$

Appendix 3 (cont.): Lateral Transfer Functions

$$YDR := q \cdot s \cdot \frac{CYDR}{w}$$

$$LB := q \cdot s \cdot b \cdot \frac{CLB}{I_{xx}}$$

$$LP := q \cdot s \cdot b \cdot \frac{2 \cdot CLP}{2 \cdot I_{xx} \cdot U1}$$

$$LR := q \cdot s \cdot b \cdot \frac{2 \cdot CLR}{2 \cdot I_{xx} \cdot U1}$$

$$LDA := q \cdot s \cdot b \cdot \frac{CLDA}{I_{xx}}$$

$$LDR := q \cdot s \cdot b \cdot \frac{CLDR}{I_{xx}}$$

$$NB := q \cdot s \cdot b \cdot \frac{CNB}{I_{zz}}$$

$$NTB := q \cdot s \cdot b \cdot \frac{CNTB}{I_{zz}}$$

$$NP := q \cdot s \cdot b \cdot \frac{2 \cdot CNP}{2 \cdot I_{zz} \cdot U1}$$

$$NR := q \cdot s \cdot b \cdot \frac{2 \cdot CNR}{2 \cdot I_{zz} \cdot U1}$$

$$NDA := q \cdot s \cdot b \cdot \frac{CNDA}{I_{zz}}$$

$$NDR := q \cdot s \cdot b \cdot \frac{CNDR}{I_{zz}}$$

Appendix 3 (cont.): Lateral Transfer Functions

YB = -32.303

YP = -0.315

YR = 1.789

YDA = 0

YDR = 19.486

LB = -28.768

LP = -12.417

LR = 2.536

LDA = 57.536

LDR = 4.752

NB = 10.126

NTB = 0

NP = -0.382

NR = -1.261

NDA = -8.257

NDR = -10.235

Lateral-Directional Transfer Functions

$$A1 := \frac{I_{xz}}{I_{xx}}$$

$$B1 := \frac{I_{xz}}{I_{zz}}$$

Denominator Polynomial

AD2 := U1 · (1 - A1 · B1)

Appendix 3 (cont.): Lateral Transfer Functions

$$BD2 := -YB \cdot (1 - A1 \cdot B1) - U1 \cdot (LP + NR + A1 \cdot NP + B1 \cdot LR)$$

$$CD21 := U1 \cdot (LP \cdot NR - LR \cdot NP) + YB \cdot (NR + LP + A1 \cdot NP + B1 \cdot LR)$$

$$CD22 := YP \cdot (LB + NB \cdot A1 + NTB \cdot A1) - U1 \cdot (LB \cdot B1 + NB + NTB)$$

$$CD23 := YR \cdot (LB \cdot B1 + NB + NTB)$$

$$CD2 := CD21 - CD22 - CD23$$

$$DD21 := -YB \cdot (LP \cdot NR - LR \cdot NP) + YP \cdot (LB \cdot NR - NB \cdot LR - NTB \cdot LR)$$

$$DD22 := -g \cdot \cos(\theta) \cdot (LB + NB \cdot A1 + NTB \cdot A1)$$

$$DD23 := U1 \cdot (LB \cdot NP - NB \cdot LP - NTB \cdot LP)$$

$$DD24 := -YR \cdot (LB \cdot NP - NB \cdot LP - NTB \cdot LP)$$

$$DD2 := DD21 + DD22 + DD23 + DD24$$

$$ED2 := g \cdot \cos(\theta) \cdot (LB \cdot NR - NB \cdot LR - NTB \cdot LR)$$

$$AD2 = 219 \qquad BD2 = 3.028 \cdot 10^3 \qquad CD2 = 6.272 \cdot 10^3$$

$$DD2 = 3.116 \cdot 10^4 \qquad ED2 = 340.735$$

$$f(s) := AD2 \cdot s^4 + BD2 \cdot s^3 + CD2 \cdot s^2 + DD2 \cdot s + ED2$$

$$s := -1 \qquad s := \text{root}(f(s), s) \qquad s = -0.011$$

$$s := -.5 + 3i \qquad s := \text{root}(f(s), s) \qquad s = -0.686 + 3.307i$$

$$s := -.5 - 3i \qquad s := \text{root}(f(s), s) \qquad s = -0.686 - 3.307i$$

$$s := -10 \qquad s := \text{root}(f(s), s) \qquad s = -12.442$$

Appendix 3 (cont.): Lateral Transfer Functions

Equations due to Aileron deflection

Numerator for β/δ_a transfer function

$$A_\beta := YDA \cdot (1 - A1 \cdot B1)$$

$$B_{\beta 1} := -YDA \cdot (NR + LP + A1 \cdot NP + B1 \cdot LR) + YP \cdot (LDA + NDA \cdot A1)$$

$$B_{\beta 2} := YR \cdot (LDA \cdot B1 + NDA) - U1 \cdot (LDA \cdot B1 + NDA)$$

$$B_\beta := B_{\beta 1} + B_{\beta 2}$$

$$C_{\beta 1} := YDA \cdot (LP \cdot NR - NP \cdot LR) + YP \cdot (NDA \cdot LR - LDA \cdot NR)$$

$$C_{\beta 2} := g \cdot \cos(\theta) \cdot (LDA + NDA \cdot A1) + YR \cdot (LDA \cdot NP - NDA \cdot LP)$$

$$C_{\beta 3} := -U1 \cdot (LDA \cdot NP - NDA \cdot LP)$$

$$C_\beta := C_{\beta 1} + C_{\beta 2} + C_{\beta 3}$$

$$D_\beta := g \cdot \cos(\theta) \cdot (NDA \cdot LR - LDA \cdot NR)$$

$$A_\beta = 0 \qquad C_\beta = 2.888 \cdot 10^4$$

$$B_\beta = 1.775 \cdot 10^3 \qquad D_\beta = 1.661 \cdot 10^3$$

$$f(s) := A_\beta \cdot s^3 + B_\beta \cdot s^2 + C_\beta \cdot s + D_\beta$$

$$s := -1 \qquad s := \text{root}(f(s), s) \qquad s = -0.058$$

$$s := -10 \qquad s := \text{root}(f(s), s) \qquad s = -16.21$$

Appendix 3 (cont.): Lateral Transfer Functions

Numerator for $\phi/\delta a$ transfer function

$$A\phi := U1 \cdot (LDA + NDA \cdot A1)$$

$$B\phi1 := U1 \cdot (NDA \cdot LR - LDA \cdot NR) - YB \cdot (LDA + NDA \cdot A1)$$

$$B\phi2 := YDA \cdot (LB + NB \cdot A1 + NTB \cdot A1)$$

$$B\phi := B\phi1 + B\phi2$$

$$C\phi1 := -YB \cdot (NDA \cdot LR - LDA \cdot NR) + YDA \cdot (LR \cdot NB + LR \cdot NTB - NR \cdot LB)$$

$$C\phi2 := (U1 - YR) \cdot (NB \cdot LDA + NTB \cdot LDA - LB \cdot NDA)$$

$$C\phi := C\phi1 + C\phi2$$

$$A\phi = 1.26 \cdot 10^4 \quad B\phi = 1.316 \cdot 10^4 \quad C\phi = 7.662 \cdot 10^4$$

$$f(s) := A\phi \cdot s^2 + B\phi \cdot s + C\phi$$

$$s := -5 - i \quad s := \text{root}(f(s), s) \quad s = -0.522 - 2.41i$$

$$s := -5 + i \quad s := \text{root}(f(s), s) \quad s = -0.522 + 2.41i$$

Numerator for $\psi/\delta a$ transfer function

$$A\psi := U1 \cdot (NDA + LDA \cdot B1)$$

$$B\psi1 := U1 \cdot (LDA \cdot NP - NDA \cdot LP) - YB \cdot (NDA + LDA \cdot B1)$$

$$B\psi2 := YDA \cdot (LB \cdot B1 + NB + NTB)$$

$$B\psi := B\psi1 + B\psi2$$

Appendix 3 (cont.): Lateral Transfer Functions

```

Cpsi1 := -YB'(LDA·NP - NDA·LP)
Cpsi2 := YP'(NB'LDA + NTB'LDA - LB·NDA)
Cpsi3 := YDA'(LB·NP - NB·LP - NTB·LP)
Cpsi := Cpsi1 + Cpsi2 + Cpsi3

```

```

Dpsi := g'cos(θ)·(NB'LDA + NTB'LDA - LB·NDA)

```

```

Apsi = -1.808·103
Cpsi = -4.131·103
Bpsi = -2.753·104
Dpsi = 1.111·104

```

```

f(s) := Apsi·s3 + Bpsi·s2 + Cpsi·s + Dpsi

```

```

s := -1.5      s := root(f(s),s)      s = -0.735
s := 1         s := root(f(s),s)      s = 0.556
s := -25      s := root(f(s),s)      s = -15.048

```

Appendix 3 (cont.): Lateral Transfer Functions

Equations due to Rudder deflection

Numerator for $\beta/\delta r$ transfer function

$$A\beta := YDR \cdot (1 - A1 \cdot B1)$$

$$B\beta_1 := -YDR \cdot (NR + LP + A1 \cdot NP + B1 \cdot LR) + YP \cdot (LDR + NDR \cdot A1)$$

$$B\beta_2 := YR \cdot (LDR \cdot B1 + NDR) - U1 \cdot (LDR \cdot B1 + NDR)$$

$$B\beta := B\beta_1 + B\beta_2$$

$$C\beta_1 := YDR \cdot (LP \cdot NR - NP \cdot LR) + YP \cdot (NDR \cdot LR - LDR \cdot NR)$$

$$C\beta_2 := g \cdot \cos(\theta) \cdot (LDR + NDR \cdot A1)$$

$$C\beta_3 := YR \cdot (LDR \cdot NP - NDR \cdot LP) - U1 \cdot (LDR \cdot NP - NDR \cdot LP)$$

$$C\beta := C\beta_1 + C\beta_2 + C\beta_3$$

$$D\beta := g \cdot \cos(\theta) \cdot (NDR \cdot LR - LDR \cdot NR)$$

$$A\beta = 19.486 \qquad C\beta = 2.848 \cdot 10^4$$

$$B\beta = 2.488 \cdot 10^3 \qquad D\beta = -643.024$$

$$f(s) := A\beta \cdot s^3 + B\beta \cdot s^2 + C\beta \cdot s + D\beta$$

$$s := 1 \qquad s := \text{root}(f(s), s) \qquad s = 0.023$$

$$s := -20 \qquad s := \text{root}(f(s), s) \qquad s = -12.738$$

$$s := -100 \qquad s := \text{root}(f(s), s) \qquad s = -114.977$$

Appendix 3 (cont.): Lateral Transfer Functions

Numerator for $\phi/\delta r$ transfer function

$$A\phi := U1 \cdot (LDR + NDR \cdot A1)$$

$$B\phi1 := U1 \cdot (NDR \cdot LR - LDR \cdot NR) - YB \cdot (LDR + NDR \cdot A1)$$

$$B\phi2 := YDR \cdot (LB + NB \cdot A1 + NTB \cdot A1)$$

$$B\phi := B\phi1 + B\phi2$$

$$C\phi1 := -YB \cdot (NDR \cdot LR - LDR \cdot NR) + YDR \cdot (LR \cdot NB + LR \cdot NTB - NR \cdot LB)$$

$$C\phi2 := (U1 - YR) \cdot (NB \cdot LDR + NTB \cdot LDR - LB \cdot NDR)$$

$$C\phi := C\phi1 + C\phi2$$

$$A\phi = 1.041 \cdot 10^3 \quad B\phi = -4.78 \cdot 10^3 \quad C\phi = -5.436 \cdot 10^4$$

$$f(s) := A\phi \cdot s^2 + B\phi \cdot s + C\phi$$

$$s := -1 \quad s := \text{root}(f(s), s) \quad s = -5.287$$

$$s := 10 \quad s := \text{root}(f(s), s) \quad s = 9.881$$

Numerator for $\psi/\delta r$ transfer function

$$A\psi := U1 \cdot (NDR + LDR \cdot B1)$$

$$B\psi1 := U1 \cdot (LDR \cdot NP - NDR \cdot LP) - YB \cdot (NDR + LDR \cdot B1)$$

$$B\psi2 := YDR \cdot (LB \cdot B1 + NB + NTB)$$

$$B\psi := B\psi1 + B\psi2$$

Appendix 3 (cont.): Lateral Transfer Functions

```

Cpsi1 := -YB'(LDR·NP - NDR·LP)
Cpsi2 := YP'(NB·LDR + NTB·LDR - LB·NDR)
Cpsi3 := YDR'(LB·NP - NB·LP - NTB·LP)
Cpsi := Cpsi1 + Cpsi2 + Cpsi3

```

```

Dpsi := g·cos(θ)·(NB·LDR + NTB·LDR - LB·NDR)

```

```

Apsi = -2.241·103          Cpsi = -1.422·103

```

```

Bpsi = -2.836·104          Dpsi = -7.932·103

```

```

f(s) := Apsi·s3 + Bpsi·s2 + Cpsi·s + Dpsi

```

```

s := -1 + i      s := root(f(s),s)      s = -0.014 + 0.529i
s := -1 - i      s := root(f(s),s)      s = -0.014 - 0.529i
s := -10         s := root(f(s),s)      s = -12.626

```

VITA

Douglas E. Wolfe

9/22/61

In 1983, the student received a bachelor of science degree in Mechanical Engineering from the University of Southern California. He began his work towards a masters degree in the winter of 1985. His course work included mechanical, electrical, and systems engineering classes with an emphasis in control system design. As of the spring of 1990, the student has completed all classes required to receive a Master of Science degree in Systems Engineering.

Professional experience has included engineering work in both the private and public sectors. After receiving his undergraduate degree, he worked for Rockwell International for one year as a project manager overseeing turbo pump design and testing for the space shuttle main engines. For the last five years he has worked for the Central Intelligence Agency as a project manager.

Signed: Douglas E Wolfe 2/1/90
Douglas E. Wolfe 2/1/90